Int. J. Solids Structures, 1971, Vol. 7, pp. 751 to 787. Pergamon Press. Printed in Great Britain

LATTICE THEORY OF FACE-SHEAR AND THICKNESS-TWIST WAVES IN B.C.C. CRYSTAL PLATES

CHUNG GONG

Department of Civil Engineering, Columbia University, New York, N.Y.

Abstract—An analytical study is made of face-shear and thickness-twist waves propagating along the [100] and [110] directions of a b.c.c. lattice plate bounded by a pair of (001) surfaces. The behavior of the waves in the [110] direction is similar to that found previously for analogous waves in the [100] direction of simple-cubic and f.c.c. plates. In the [100] direction of the b.c.c. plate, the situation is quite different. Near the halfway point of the first Brillouin zone, the lowest symmetric mode and the lowest antisymmetric mode are predominantly surface modes and the remaining modes group together in a narrow, high frequency band-pass. The results of numerical computations are exhibited for iron and tungsten.

INTRODUCTION

FACE-SHEAR and thickness-twist waves in lattice plates have been previously investigated by Mindlin [1] and by Brady [2]. Mindlin examined simple cubic lattices and showed that the character of face-shear and thickness-twist modes in such lattices differed from that exhibited in continuum plates, the essential difference being two-fold: first, the number of modes for each value of the wave-length was equal to the number of layers in the case of a lattice plate, whereas it is infinite in the case of a continuum plate; and, second, the lattice plate exhibited the usual character associated with a periodic structure; namely, the existence of Brillouin zones and a dispersion associated with the lattice constant in addition to that associated with the finite thickness of the plate.

Brady [2] investigated waves along the [100] direction of a f.c.c. lattice plate. His results did not show any striking differences from those of Mindlin [1]. The overall character of the dispersion curves obtained by Brady were almost indistinguishable from those of the simple cubic lattice. The only difference appeared in the variation of displacements across the thickness. Brady's results were influenced by the inclusion of interactions between particles lying on next-nearest layers. As a result, the variation of the displacements across the thickness was not sinusoidal as in the case of the simple cubic lattice examined by Mindlin, where only nearest-layer interactions were included. There was an additional component of displacement which was confined near the bounding surfaces of the plate. However, the amplitude of this surface component was small and did not influence appreciably the overall pattern of displacements.

In this paper, we have considered face-shear and thickness-twist waves propagating along the [100] and [110] directions of a b.c.c. crystal lattice plate bounded by two (001) surfaces. We have used the four-constant lattice model of Clark *et al.* [3]. This model includes nearest and next-nearest neighbor central-force interactions and two angular-stiffness interactions. These interactions involve up to sixth order difference operators in the equations of motion. The corresponding force constants were chosen so that the long

wave approximation and one point in the dispersion relation at the first Brillouin boundary match experimental results.

Our results for waves along the [110] direction are very similar to those for waves along the [100] direction of an f.c.c. lattice plate [2]. This is not surprising, because the geometric arrangement of the particles of a b.c.c. lattice viewed from a [110] direction resembles that of an f.c.c. lattice, the only difference being one of a distortion of scale in one direction.

However, the results for waves along the [100] direction are strikingly different. First, for most materials, all but two of the dispersion curves appear to coalesce at the halfway point of the first Brillouin zone. And, second, the lowest two branches have strong surface components which become predominant at short wave lengths but which survive even at moderately long wave lengths in the lowest symmetric branch. The possibility of existence of surface waves of other than the Rayleigh type has been mentioned previously by Feuchtwang [4] and confirmed by the computations of Allen *et al.* [5], who found some non-Rayleigh surface modes near the first Brillouin zone boundary on (111) surfaces of f.c.c. lattices. Here we report the existence of two non-Rayleigh surface modes of pure shear on (001) surfaces of b.c.c. lattices and give a detailed investigation of the displacements associated with them.

The coalescing of the higher modes halfway into the Brillouin zone is a direct consequence of the band structure corresponding to the (010) plane of the Brillouin zone. For most materials, the band-width of transverse shear waves is very small at this halfway point. In the framework of the lattice model used, this band-width diminishes to zero as the angular-stiffness force constant tends to zero. In that case the elastic constants satisfy the Cauchy relation which, for cubic crystals, is simply $C_{44} = C_{12}$. We have examined two materials one of which, iron, almost satisfies the Cauchy relation. The other material, tungsten, is very nearly isotropic; i.e. its elastic constants almost satisfy the condition $C_{11} - C_{12} - 2C_{44} = 0$. There is very little qualitative difference between the results for these two materials other than that in the case of iron the coalescing of the dispersion branches for waves in the [100] direction is more pronounced.

BASIC EQUATIONS

We use the equations of motion for a monatomic b.c.c. lattice given by Clark *et al.* [3]. These equations, repeated here for ease of reference, include up to sixth order difference operators and are the following

$$\begin{aligned} M\ddot{u}_j = {} & \tfrac{3}{2}(2\gamma_1+\gamma_2)U_j^j + (\alpha-\gamma_1+\tfrac{3}{2}\gamma_2)\sum_{s=1}^{3} U_j^s \\ & + \left[(\beta+4\gamma_1)\sum_{P_{1j}} + (-\gamma_1+\tfrac{3}{2}\gamma_2)\sum_{P_{2j}}\right] u_j^{l+\xi,m+\eta,n+\zeta} \\ & - (8\alpha+2\beta+20\gamma_1+30\gamma_2)u_j^{l,m,n} \end{aligned} \tag{1}$$

where

$$U_j^k = \lambda_j \sum_P \lambda_k u_k^{l+\xi,m+\eta,n+\zeta}, \qquad \lambda_1 = \xi, \qquad \lambda_2 = \eta, \qquad \lambda_3 = \zeta; \qquad j,k = 1,2,3 \tag{2}$$

and P, P_{1j}, P_{2j} are the point sets defined as follows:

$$
\begin{aligned}
P(\xi,\eta,\zeta) &\equiv (1,1,1;1,1,-1;1,-1,1;1,-1,-1;\\
&\qquad -1,1,1;-1,1,-1;-1,-1,1;-1,-1,-1),\\
P_{11}(\xi,\eta,\zeta) &\equiv (2,0,0;-2,0,0),\\
P_{12}(\xi,\eta,\zeta) &\equiv (0,2,0;0,-2,0),\\
P_{13}(\xi,\eta,\zeta) &\equiv (0,0,2;0,0,-2),\\
P_{21}(\xi,\eta,\zeta) &\equiv (0,2,0;0,-2,0;0,0,2;0,0,-2),\\
P_{22}(\xi,\eta,\zeta) &\equiv (0,0,2;0,0,-2;2,0,0;-2,0,0),\\
P_{23}(\xi,\eta,\zeta) &\equiv (2,0,0;-2,0,0;0,2,0;0,-2,0).
\end{aligned}
\tag{3}
$$

In equations (1) M is the mass of an atom, dots denote differentiation with respect to time; $u_j^{l,m,n}$ are the rectangular components of displacement of the atom at point l, m, n; α and β are nearest and next nearest neighbor central force constants, respectively; and γ_1 and γ_2 are angular force constants.

The boundary conditions are obtained by considering the bounded lattice domain as part of an infinite domain. The displacements near the boundary are then constrained to be such as to make the forces acting on the particles in the domain of interest from the fictitious extension equal to zero. Our domain of interest is a plate with $2N+1$ layers. Only the particles in layers $n = \pm N$ and $n = \pm(N-1)$, numbered from the center layer, are affected by the boundary conditions. These conditions are analogous to those given by Gazis and Wallis [6], the essential difference being that here we consider values of γ_2 different from zero.

For the layers $n = \pm N$, we have the conditions

$$
\begin{aligned}
&2\gamma_1\left(\sum_{R_1} u_1^{l+2\xi,m,\pm N} - 2u_1^{l,m,\pm N}\right) + \tfrac{1}{2}(-\gamma_1+\tfrac{3}{2}\gamma_2)\left(\sum_{R_2} u_1^{l,m+2\eta,\pm N} + 2u_1^{l,m,\pm(N+2)} - 4u_1^{l,m,\pm N}\right)\\
&\quad + (\alpha+2\gamma_1+3\gamma_2)\left(\sum_{R_3} u_1^{l+\xi,m+\eta,\pm(N+1)} - 4u_1^{l,m,\pm N}\right) + \tfrac{1}{4}(2\gamma_1+\gamma_2)\left[\sum_{R_3}(u_1^{l+\xi,m+\eta,\pm(N-1)}\right.\\
&\quad \left. + \xi\eta u_2^{l+\xi,m+\eta,\pm(N-1)} \pm 2\xi u_3^{l+\xi,m+\eta,\pm(N-1)}) - 4u_1^{l,m,\pm N}\right]\\
&\quad + (\alpha-\gamma_1+\tfrac{3}{2}\gamma_2)\sum_{R_3}\xi(\eta u_2^{l+\xi,m+\eta,\pm(N+1)} \pm u_3^{l+\xi,m+\eta,\pm(N+1)})\\
&\quad \pm (\gamma_1+\tfrac{3}{2}\gamma_2)\sum_{R_1}\xi u_3^{l+2\xi,m,\pm N} = 0,
\end{aligned}
\tag{4a}
$$

$$2\gamma_1\left(\sum_{R_2} u_2^{l,m+2\eta,\pm N}-2u_2^{l,m,\pm N}\right)+\tfrac{1}{2}(-\gamma_1+\tfrac{3}{2}\gamma_2)\left(\sum_{R_1} u_2^{l+2\xi,m,\pm N}+2u_2^{l,m,\pm(N+2)}-4u_2^{l,m,\pm N}\right)$$
$$+(\alpha+2\gamma_1+3\gamma_2)\left(\sum_{R_3} u_2^{l+\xi,m+\eta,\pm(N+1)}-4u_2^{l,m,\pm N}\right)+\tfrac{1}{4}(2\gamma_1+\gamma_2)\Bigg[\sum_{R_3}(u_2^{l+\xi,m+\eta,\pm(N-1)}$$
$$+\xi\eta u_1^{l+\xi,m+\eta,\pm(N-1)}\pm 2\eta u_3^{l+\xi,m+\eta,\pm(N-1)}-4u_1^{l,m,\pm N}\Bigg]$$
$$+(\alpha-\gamma_1+\tfrac{3}{2}\gamma_2)\sum_{R_3}\eta(\xi u_1^{l+\xi,m+\eta,\pm(N+1)}\pm u_3^{l+\xi,m+\eta,\pm(N+1)})$$
$$\pm(\gamma_1+\tfrac{3}{2}\gamma_2)\sum_{R_2}\eta u_3^{l,m+2\eta,\pm N}=0, \tag{4b}$$

$$\mp(\gamma_1+\tfrac{3}{2}\gamma_2)\sum_{R_{12}}(\xi u_1^{l+2\xi,m,\pm N}+\eta u_2^{l,m+2\eta,\pm N})\pm(\alpha-\gamma_1+\tfrac{3}{2}\gamma_2)\sum_{R_3}(\xi u_1^{l+\xi,m+\eta,\pm(N+1)}$$
$$+\eta u_2^{l+\xi,m+\eta,\pm(N+1)})+\gamma_2\Bigg[\sum_{R_3}(\mp\xi u_1^{l+\xi,m+\eta,\pm(N-1)}\mp\eta u_2^{l+\xi,m+\eta,\pm(N-1)}$$
$$+u_3^{l+\xi,m+\eta,\pm(N-1)})-4u_3^{l,m,\pm N}\Bigg]+\tfrac{1}{2}(-\gamma_1+\tfrac{3}{2}\gamma_2)\left(\sum_{R_{12}} u_3^{l+2\xi,m+2\eta,\pm N}-4u_3^{l,m,\pm N}\right)$$
$$+(\beta+4\gamma_1)(u_3^{l,m,\pm(N+2)}-u_3^{l,m,\pm N})$$
$$+(\alpha+2\gamma_1+3\gamma_2)\left(\sum_{R_3} u_3^{l+\xi,m+\eta,\pm(N+1)}-4u_3^{l,m,\pm N}\right)=0, \tag{4c}$$

where

$$\begin{aligned} R_1(\xi,\eta) &\equiv (1,0;-1,0),\\ R_2(\xi,\eta) &\equiv (0,1;0,-1),\\ R_{12}(\xi,\eta) &\equiv R_1(\xi,\eta)\oplus R_2(\xi,\eta)\\ &\equiv (1,0;-1,0;0,1;0,-1),\\ R_3(\xi,\eta) &\equiv (1,1;-1,1;1,-1;-1,-1). \end{aligned} \tag{5}$$

For the layers $n=\pm(N-1)$, we have the conditions

$$\tfrac{1}{4}(2\gamma_1+\gamma_2)\Bigg[\sum_{R_4}(u_1^{l+1+\xi,m+1+\eta,\pm N}+\xi\eta u_2^{l+1+\xi,m+1+\eta,\pm N})-4u_1^{l+1,m+1,\pm(N-1)}\Bigg]$$
$$+(\gamma_1-\tfrac{3}{2}\gamma_2)(u_1^{l+1,m+1,\pm(N-1)}-u_1^{l+1,m+1,\pm(N+1)})\pm\gamma_2\sum_{R_4}\xi u_3^{l+1+\xi,m+1+\eta,\pm N}=0, \tag{6a}$$

$$\tfrac{1}{4}(2\gamma_1+\gamma_2)\Bigg[\sum_{R_4}(u_2^{l+1+\xi,m+1+\eta,\pm N}+\xi\eta u_1^{l+1+\xi,m+1+\eta,\pm N})-4u_2^{l+1,m+1,\pm(N-1)}\Bigg]$$
$$+(\gamma_1-\tfrac{3}{2}\gamma_2)(u_2^{l+1,m+1,\pm(N-1)}-u_2^{l+1,m+1,\pm(N+1)})\pm\gamma_2\sum_{R_4}\eta u_3^{l+1+\xi,m+1+\eta,\pm N}=0, \tag{6b}$$

$$(\beta+4\gamma_1)(u_3^{l+1,m+1,\pm(N+1)}-u_3^{l+1,m+1,\pm(N-1)})+\gamma_2\left(\sum_{R_4} u_3^{l+1+\xi,m+1+\eta,\pm N}-4u_3^{l+1,m+1,\pm(N-1)}\right)$$
$$\mp(2\gamma_1+\gamma_2)\sum_{R_4}(\xi u_1^{l+1+\xi,m+1+\eta,\pm N}+\eta u_2^{l+1+\xi,m+1+\eta,\pm N})=0, \tag{6c}$$

where

$$R_4(\xi, \eta) \equiv (-1, -1; 1, -1; -1, 1; 1, 1). \tag{7}$$

The relation between the force constants and the elastic constants of the corresponding continuum resulting from long wave approximation has been obtained in [3] and is given by

$$\begin{aligned} aC_{11} &= \alpha+\beta+6\gamma_1+3\gamma_2, \\ aC_{12} &= \alpha-3\gamma_1-\tfrac{3}{2}\gamma_2, \\ aC_{44} &= \alpha+\gamma_1+\tfrac{9}{2}\gamma_2. \end{aligned} \tag{8}$$

Here, $2a = h$ is the atomic distance between the next nearest neighbors, while in [3] a was taken equal to h.

In order to determine uniquely the four lattice force constants, another relationship is needed. This relation may be derived by matching some critical frequency obtained by direct calculation from the equations of motion with that obtained experimentally. Setting

$$\gamma_2 = q\gamma_1, \tag{9}$$

we find that the dispersion relations for the [110] direction are independent of q, whereas for the [100] direction, both the longitudinal and the transverse branches are functions of q. These two branches, for the direction [100], intersect at the end of the first Brillouin zone according to both the theoretical derivation and experimental results. The parameter q is used to match this intersection point of the dispersion curves. If $\omega_E(\pi)$ denotes the experimental value of frequency at the intersection point, we find

$$q = \frac{2\left[(5C_{44}-C_{12})-\dfrac{M\omega_E^2(\pi)}{4a}\right]}{3\left[\dfrac{M\omega_E^2(\pi)}{4a}-(C_{12}+3C_{44})\right]} \tag{10}$$

Note that the limiting velocities of propagation of the longitudinal and the transverse waves at $\omega = 0$, $\theta_1 = 0$ are independent of q, hence they are not affected by the above equation. Note also that theoretically [from equations (1)] as well as experimentally it can be shown that $\omega_E(\pi)$ is a relative extremal but not necessarily the maximum.

FACE-SHEAR AND THICKNESS-TWIST WAVES IN THE [100] DIRECTION

The displacement field for the thickness-twist waves in the [100] direction has the form

$$\begin{aligned} u_1^{l,m,n} &= u_3^{l,m,n} = 0, \\ u_2^{l,m,n} &= B\exp[i(\theta_1 l+\theta_3 n-\omega t)], \\ 0 &\le \theta_1 \le \pi, \qquad 0 \le \operatorname{Re}\theta_3 \le \pi. \end{aligned} \tag{11}$$

Upon substituting this displacement field into the equations of motion (1), we obtain

$$\begin{aligned} &2(-2\gamma_1+3\gamma_2)(\cos^2\theta_1+\cos^2\theta_3)+8(\alpha+2\gamma_1+3\gamma_2)\cos\theta_1\cos\theta_3 \\ &\quad +M\omega^2-4(2\alpha+2\gamma_1+9\gamma_2) = 0, \end{aligned} \tag{12}$$

where θ_1 and θ_3 are dimensionless wave numbers in the directions [100] and [001] respectively. Equation (12) is a quadratic equation in $\cos\theta_3$ as well as $\cos\theta_1$. For a fixed wave number θ_1 in the [100] direction we find two roots for $\cos\theta_3$ or θ_3. Using the relations (8) we may solve for $\cos\theta_{3k}$ from (12) and obtain

$$\begin{matrix}\cos\theta_{31}\\ \cos\theta_{32}\end{matrix} = \frac{1}{(2-3q)(C_{12}-C_{44})}\left\{[3(2+q)(C_{12}-C_{44})-2(2+3q)(C_{12}+C_{44})]\cos\theta_1 \right.$$
$$\left. \pm\left[(4-9q^2)(C_{12}-C_{44})\frac{M}{a}(\omega_m^2-\omega^2)\right]^{\frac{1}{2}}\right\}, \tag{13}$$

where

$$\frac{M}{a}\omega_m^2 = 8C_{44}\left\{\frac{1}{2-3q}\left[\frac{2(2+3q)C_{12}}{C_{12}-C_{44}}-3(2+q)\right]\cos^2\theta_1+1\right\}. \tag{14}$$

Thus the displacement field in a plate reduces to the form

$$u_1^{l,m,n} = u_3^{l,m,n} = 0,$$
$$u_2^{l,m,n} = \sum_{k=1}^{2}(B_{1k}\cos\theta_{3k}n + B_{2k}\sin\theta_{3k}n)\,e^{i(\theta_1 l-\omega t)}. \tag{15}$$

The eigenfrequencies of the lattice plate, and the corresponding θ_{3k}, are to be determined by using the boundary conditions. However, certain statements concerning these frequencies can be made by recalling Rayleigh's theorem [7] on the effect of relaxation of spring constants. The argument goes as follows:

In an infinite domain all frequencies of propagating modes lie within a "passing band". For any value of θ_1 the passing band is such that at least one of the θ_{3k} is real. Introduction of a free boundary amounts to a reduction of elastic (spring) constants. By Rayleigh's theorem it lowers all frequencies, and may produce an eigenfrequency below the passing band. Such a frequency would correspond to a surface mode. It will be seen that the introduction of two free surfaces causes as many as two surface modes to appear. Most of the modes, however, lie within the passing band. Therefore, it is instructive to investigate the shape of this band as θ_1 varies between 0 and π. Equation (12) may be written in the form

$$\frac{M\omega^2}{a} = 8C_{44}-\frac{2-3q}{2+3q}(C_{12}-C_{44})(\cos^2\theta_1+\cos^2\theta_3)$$
$$-\frac{2}{2+3q}[2(2+3q)(C_{12}+C_{44})-3(2+q)(C_{12}-C_{44})]\cos\theta_1\cos\theta_3. \tag{16}$$

Partial differentiation with respect to θ_3 yields

$$\frac{\partial\omega}{\partial\theta_3} = \frac{a}{\omega M(2+3q)}\sin\theta_3\{(2-3q)(C_{12}-C_{44})\cos\theta_3$$
$$+[2(2+3q)(C_{12}+C_{44})-3(2+q)(C_{12}-C_{44})]\cos\theta_1\}. \tag{17}$$

The relative extreme values of ω for $\omega \neq 0$ are at

$$\theta_3 = 0, \pi, \tag{18}$$

and also at

$$\theta_3 = \arccos\left\{-\frac{[2(2+3q)(C_{12}+C_{44})-3(2+q)(C_{12}-C_{44})]\cos\theta_1}{(2-3q)(C_{12}-C_{44})}\right\} \equiv \theta_{3m}, \quad (19a)$$

provided that

$$|\cos\theta_1| < \left|\frac{(2-3q)(C_{12}-C_{44})}{2(2+3q)(C_{12}+C_{44})-3(2+q)(C_{12}-C_{44})}\right|. \quad (19b)$$

Otherwise one finds that for real θ_3 the relative minimum frequency is at $\theta_3 = 0$, and the relative maximum frequency at $\theta_3 = \pi$. Thus for

$$|\cos\theta_1| > \left|\frac{(2-3q)(C_{12}-C_{44})}{2(2+3q)(C_{12}+C_{44})-3(2+q)(C_{12}-C_{44})}\right|, \quad (20)$$

we find, for $0 \leq \theta_1 < \pi/2$

$$\begin{aligned}\frac{\omega_{\min}}{\omega_{\max}} = \left[\frac{a}{M(2+3q)}\right]^{\frac{1}{2}} &\{4(2+3q)(C_{12}+C_{44})-(10+9q)(C_{12}-C_{44}) \\ &-(2-3q)(C_{12}-C_{44})\cos^2\theta_1 \\ &\mp 2[2(2+3q)(C_{12}+C_{44})-3(2+q)(C_{12}-C_{44})]\cos\theta_1\}^{\frac{1}{2}}. \end{aligned} \quad (21)$$

Furthermore, assuming $C_{44} < C_{12}$ we find that

$$\omega(\theta_{3m}) = \begin{cases}\omega_{\max} \text{ and } \omega(0) = \omega_{\min}, \text{ for } 0 < |q| < \frac{2}{3}, \\ \omega_{\min} \text{ and } \omega(\pi) = \omega_{\max}, \text{ for } \frac{2}{3} < |q|. \end{cases} \quad (22)$$

For instance at $\theta_1 = \pi/2$, $\cos\theta_1 = 0$ and equations (19) are satisfied, hence we find

$$\begin{aligned}\theta_3 = \theta_{3m} &= \frac{\pi}{2}, \\ \omega\left(\frac{\pi}{2}\right) &= 2\left(\frac{2aC_{44}}{M}\right)^{\frac{1}{2}}, \\ \omega(\pi) &= \omega(0) \\ &= \left\{\frac{a}{M}\left[8C_{44}-\frac{(2-3q)(C_{12}-C_{44})}{2+3q}\right]\right\}^{\frac{1}{2}}. \end{aligned} \quad (23)$$

The width of the passing band, $(\omega_{\max}-\omega_{\min})$, at $\theta_1 = \pi/2$, for example, with $C_{44} < C_{12}$ and $|q| < \frac{2}{3}$, is

$$\begin{aligned}\omega_{\max}-\omega_{\min} &= \omega\left(\frac{\pi}{2}\right)-\omega(0) \\ &= 2\left(\frac{2aC_{44}}{M}\right)^{\frac{1}{2}}\left\{1-\left[1-\frac{2-3q}{8(2+3q)}\left(\frac{C_{12}}{C_{44}}-1\right)\right]^{\frac{1}{2}}\right\}. \end{aligned} \quad (24)$$

In the case

$$\frac{2-3q}{8(2+3q)}\left(\frac{C_{12}}{C_{44}}-1\right) \ll 1,$$
$$\omega_{\max}-\omega_{\min} \cong \left(\frac{2aC_{44}}{M}\right)^{\frac{1}{2}}\left[\frac{2-3q}{8(2+3q)}\left(\frac{C_{12}}{C_{44}}-1\right)\right]. \tag{25}$$

In the cases $q = \frac{2}{3}$ and $\gamma_1 = \gamma_2 = C_{12}-C_{44} = 0$, equation (12) degenerates to a linear equation in $\cos\theta_3$, hence there is only one wave number in the direction of the thickness of the plate for each ω. In that case the width of the passing band at $\theta_1 = \pi/2$ reduces to zero.

Let us now investigate the nature of the wave numbers θ_{3k} for values of ω outside of the passing band. In that case, either $\cos\theta_{3k}$ are real but with absolute value greater than 1, or $\cos\theta_{3k}$ are complex conjugate. The latter case obtains when

$$(4-9q^2)(C_{12}-C_{44})\frac{M}{a}(\omega_m^2-\omega^2) < 0. \tag{26}$$

Let

$$D_m(\theta_1) = (4-9q^2)(C_{12}-C_{44})\frac{M}{a}\omega_m^2. \tag{27}$$

Then, by using the value ω_m^2 obtained from equation (14) we find

$$D_m(\theta_1) = 8C_{44}(2+3q)\{[(2+3q)(C_{12}+C_{44})-4(C_{12}-C_{44})]\cos^2\theta_1 + (2-3q)(C_{12}-C_{44})\}. \tag{28}$$

Hence, $D_m(\theta_1) > 0$, for $0 \le \theta_1 \le \pi$ if $C_{44} < C_{12}$ and $|q| < \frac{2}{3}$ i.e. $\cos\theta_{3k}$ are real for $0 \le \omega^2 \le \omega_m^2$. And $D_m(\theta_1) < 0$ for

$$|\cos\theta_1| < \left|\frac{(2-3q)(C_{12}-C_{44})}{(2+3q)(C_{12}+C_{44})-4(C_{12}-C_{44})}\right|^{\frac{1}{2}} \tag{29}$$

if $C_{44} < C_{12}$ and $|q| > \frac{2}{3}$. In this case, the $\cos\theta_{3k}$ become complex for $0 \le \omega^2 \le \omega_m^2$.

The variation of ω vs. θ_3, for several values of θ_1, is shown in Figs. 1–3 for $|q| < \frac{2}{3}$ and Figs. 4–6 for $|q| > \frac{2}{3}$.

For an infinite lattice plate with a finite number of atoms across the thickness, the number of fundamental mode shapes of vibration is finite and is equal to the number of atomic layers across the thickness. In other words, for each value of θ_1 there is only a finite number of frequencies, and corresponding θ_{3k}, which satisfy the traction-free boundary conditions on both faces of a lattice plate with a finite thickness. If the number of layers across the thickness is odd, the lattice coordinate numbers, l, m, n, in the equations (1), (2), (4), (6), (11), (15) are integers (including zero), whereas if the number of layers across the thickness is even, then the numbers l, m, n must be odd multiples of (1/2), i.e. $\pm\frac{1}{2}(2p+1)$, where p is an integer. This difference in l, m, n has no effect on the equations of motion and consequently equation (12) remains unchanged. Nevertheless the boundary conditions will be changed since, when the number of layers is odd, the geometric configuration is symmetric about the middle plane while, when the number of layers is even, the geometric configuration is no longer symmetric about the fictitious middle plane. However, the dispersion curves

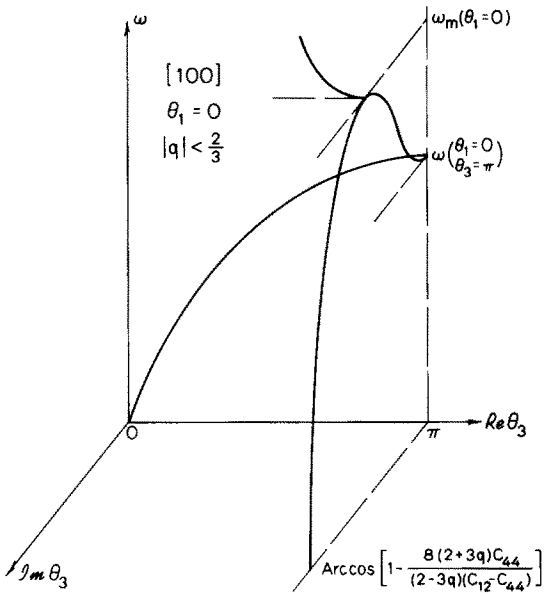

$$\omega_m(\theta_1 = 0) = 4\left[\frac{a(2+3q)}{M(2-3q)(C_{12}-C_{44})}\right]^{1/2} C_{44}$$

$$\omega\left(\begin{matrix}\theta_1 = 0\\ \theta_3 = \pi\end{matrix}\right) = 2\sqrt{\frac{a}{M}}\left[2(C_{12}+C_{44}) - \frac{3(2+q)}{2+3q}(C_{12}-C_{44})\right]^{1/2}$$

FIG. 1. The variation of ω vs. θ_3, for SH-waves along the [100] direction, with $\theta_1 = 0$ and $|q| < \frac{2}{3}$.

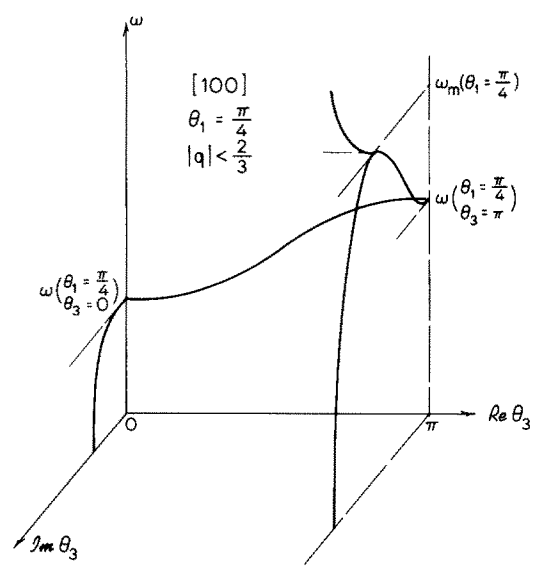

FIG. 2. The variation of ω vs. θ_3, for SH-waves along the [100] direction, with $\theta_1 = \pi/4$ and $|q| < \frac{2}{3}$.

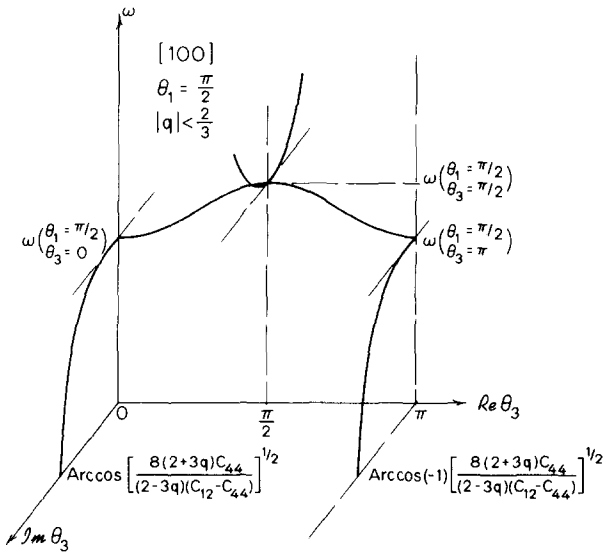

FIG. 3. The variation of ω vs. θ_3, for SH-waves along the [100] direction, with $\theta_1 = \pi/2$ and $|q| < \frac{2}{3}$.

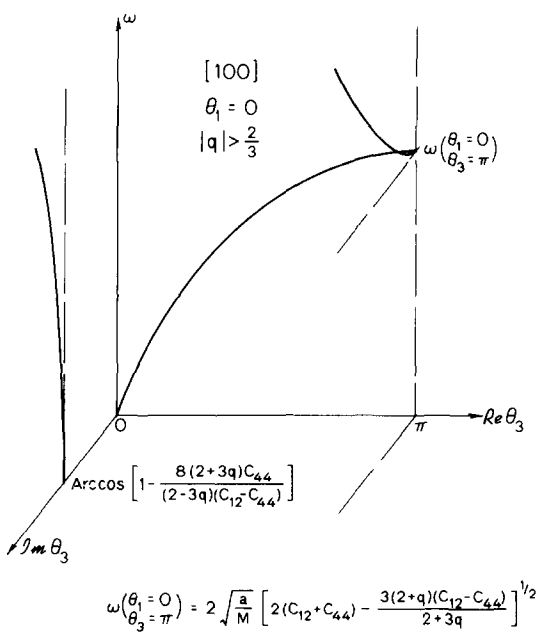

FIG. 4. The variation of ω vs. θ_3, for SH-waves along the [100] direction, with $\theta_1 = 0$ and $|q| > \frac{2}{3}$.

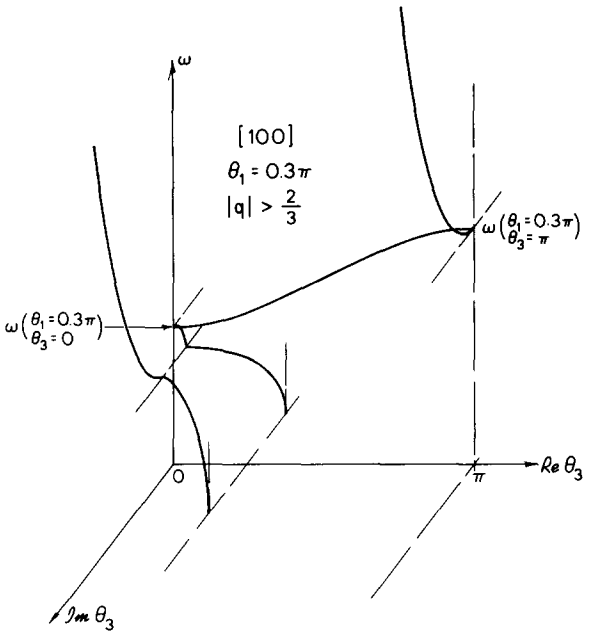

FIG. 5. The variation of ω vs. θ_3, for *SH*-waves along the [100] direction, with $\theta_1 = 0{\cdot}3\pi$ and $|q| > \frac{2}{3}$.

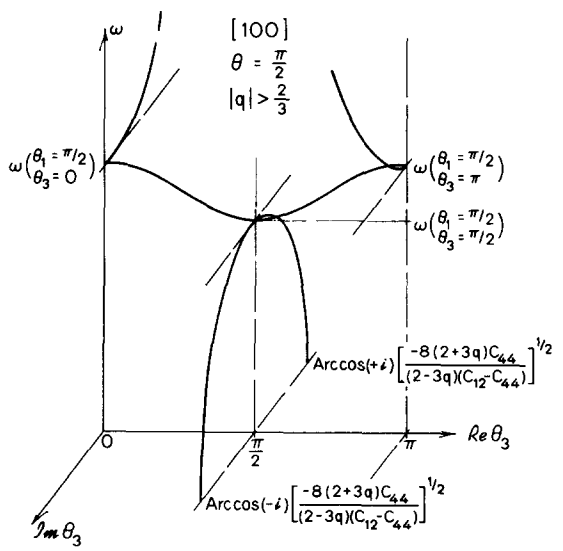

$$\omega\left(\begin{matrix}\theta_1 = \pi/2\\ \theta_3 = \pi/2\end{matrix}\right) = 2\sqrt{\frac{2aC_{44}}{M}}$$

$$\omega\left(\begin{matrix}\theta_1 = \pi/2\\ \theta_3 = 0\end{matrix}\right) = \omega\left(\begin{matrix}\theta_1 = \pi/2\\ \theta_3 = \pi\end{matrix}\right) = \sqrt{\frac{a}{M}}\left[8C_{44} - \frac{(2-3q)(C_{12}-C_{44})}{2+3q}\right]^{1/2}$$

FIG. 6. The variation of ω vs. θ_3, for *SH*-waves along the [100] direction, with $\theta_1 = \pi/2$ and $|q| > \frac{2}{3}$.

of the spectrum for either an even or odd number of layers approach the same limit as the number of layers of the lattice plate increases.

In the present paper we limit our discussion to the plate of odd number of atomic layers. The boundary conditions for the faces $n = \pm N$ and $n = \pm(N-1)$ are obtained by substituting the displacement field (15) into equations (4) and (6). We thus obtain the system of linear homogeneous equations:

$$\begin{vmatrix} F_{11} & F_{12} & -G_{11} & -G_{12} \\ F_{21} & F_{22} & -G_{21} & -G_{22} \\ F_{11} & F_{12} & G_{11} & G_{12} \\ F_{21} & F_{22} & G_{21} & G_{22} \end{vmatrix} \begin{vmatrix} B_{11} \\ B_{12} \\ B_{21} \\ B_{22} \end{vmatrix} = 0, \tag{30}$$

where

$$\begin{aligned} F_{jk} &= f_{jk} \cos \theta_{3k} N - f'_{jk} \sin \theta_{3k} N, \\ G_{jk} &= f_{jk} \sin \theta_{3k} N + f'_{jk} \cos \theta_{3k} N, j, k = 1, 2; \end{aligned} \tag{31}$$

and

$$\begin{aligned} f_{1k} &= -\frac{a}{2(2+3q)}\{(2-3q)(C_{12}-C_{44})(\sin^2 \theta_1 + \sin^2 \theta_{3k}) \\ &\quad + [4(2+3q)(C_{12}+C_{44}) - 7(2+q)(C_{12}-C_{44})](1-\cos \theta_1 \cos \theta_{3k})\}, \\ f'_{1k} &= \frac{a \sin \theta_{3k}}{2(2+3q)}\{(2-3q)(C_{12}-C_{44}) \cos \theta_{3k} \\ &\quad + [4(2+3q)(C_{12}+C_{44}) - 5(2+q)(C_{12}-C_{44})] \cos \theta_1\}, \\ f_{2k} &= \frac{a}{2(2+3q)}(2+q)(C_{12}-C_{44})(\cos \theta_{3k} - \cos \theta_1), \\ f'_{2k} &= -\frac{4aq}{2(2+3q)}(C_{12}-C_{44}) \sin \theta_{3k}. \end{aligned} \tag{32}$$

For a non-trivial solution of B_{jk}, the coefficient determinant of equations (30) must vanish, viz.

$$\begin{Vmatrix} F_{11} & F_{12} & -G_{11} & -G_{12} \\ F_{21} & F_{22} & -G_{21} & -G_{22} \\ F_{11} & F_{12} & G_{11} & G_{12} \\ F_{21} & F_{22} & G_{21} & G_{22} \end{Vmatrix} = 0, \tag{33}$$

or equivalently

$$\begin{Vmatrix} F_{11} & F_{12} \\ F_{21} & F_{22} \end{Vmatrix} = 0, \quad \text{or} \quad \begin{Vmatrix} G_{11} & G_{12} \\ G_{21} & G_{22} \end{Vmatrix} = 0. \tag{34}$$

Note that the coefficient matrix **F** corresponds to B_{1k}, the symmetric modes, while **G** corresponds to B_{2k}, the antisymmetric modes.

The amplitude ratio of the pair of mode shapes across the thickness is:
for symmetric modes,

$$\frac{B_{11}}{B_{12}} = -\frac{H_{12}}{H_{11}}, \tag{35}$$

and, for antisymmetric modes,

$$\frac{B_{21}}{B_{22}} = -\frac{H_{22}}{H_{21}}, \tag{36}$$

where

$$\begin{aligned} H_{1k} &= (2+q)(\cos\theta_1 - \cos\theta_{3k})\cos\theta_{3k}N - 4q\sin\theta_{3k}\sin\theta_{3k}N, \\ H_{2k} &= (2+q)(\cos\theta_1 - \cos\theta_{3k})\sin\theta_{3k}N + 4q\sin\theta_{3k}\cos\theta_{3k}N. \end{aligned} \tag{37}$$

FACE-SHEAR AND THICKNESS-TWIST WAVES IN THE [110] DIRECTION

Viewed along the [110] direction the geometric configuration of a b.c.c. crystal lattice is quite similar to that of a f.c.c. crystal lattice, Fig. 7, or an orthorhombic F crystal lattice with $a = b = c\sqrt{2}$. Hence we may expect that the pattern of the dispersion curves for waves propagating in the [110] direction in a b.c.c. crystal lattice is similar to that of the dispersion curves for waves propagating in the [100] direction in a f.c.c. crystal lattice. This is indeed the case as will be seen in the sequel.

The displacement field for SH-waves in the [110] direction assumes the form:

$$\begin{gathered} u_j^{l,m,n} = (-1)^{j+1}\exp\{i[\theta(l+m)+\theta_3 n-\omega t]\}, \qquad u_3^{l,m,n} = 0, \\ 0 \le \theta \le \frac{\pi}{2}, \qquad 0 \le \operatorname{Re}\theta_3 \le \pi, \qquad j = 1,2. \end{gathered} \tag{38}$$

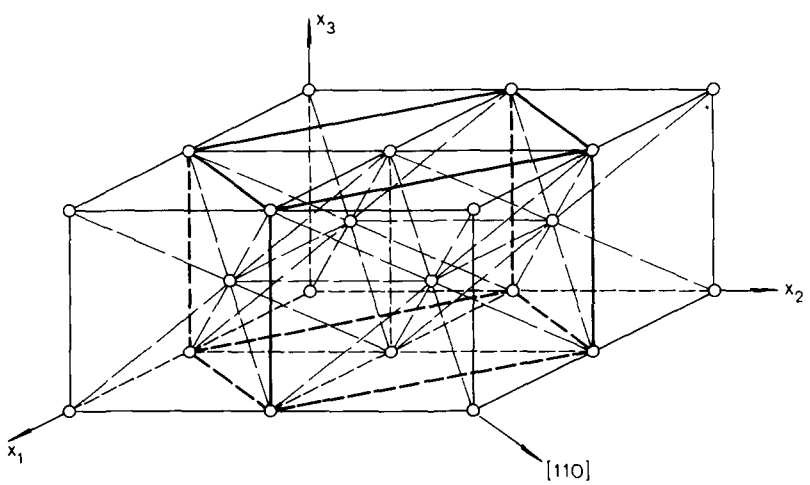

FIG. 7. A distorted f.c.c. lattice is formed in the b.c.c. lattice.

Upon substituting this displacement field into the equations of motion (1), we find

$$\begin{aligned} M\omega^2 = {} & 2[6(2\gamma_1+\gamma_2)\cos\theta_3+(2\beta+6\gamma_1+3\gamma_2)]\sin^2\theta \\ & +8(\alpha+2\gamma_1+3\gamma_2)(1-\cos\theta_3) \\ & +2(-2\gamma_1+3\gamma_2)\sin^2\theta_3. \end{aligned} \tag{39}$$

We observe that this equation is a function of $\sin^2\theta$, and therefore the dispersion curves are symmetric about $\theta = \pi/2$, where θ is the nondimensional wave number and $\theta = \pi/2$ is the end of the first Brillouin zone. Applying the relations (8), and solving equation (39) for $\cos\theta_3$, we obtain

$$\begin{aligned} \frac{\cos\theta_{31}}{\cos\theta_{32}} = \frac{1}{2-3q}\Bigg\{ & 3(2+q)\cos^2\theta - \frac{2(2+3q)(C_{12}+C_{44})}{C_{12}-C_{44}} \\ & \pm\left[\frac{4-9q^2}{C_{12}-C_{44}}\frac{M}{a}(\omega_m^2-\omega^2)\right]^{\frac{1}{2}}\Bigg\}, \end{aligned} \tag{40}$$

where

$$\begin{aligned} \frac{M\omega_m^2}{a} = \frac{1}{2-3q}\Bigg\{ & \frac{9(2+q)^2}{2+3q}(C_{12}-C_{44})\sin^4\theta \\ & +4[6(2+q)C_{44}+(2-3q)(C_{11}-C_{12})]\sin^2\theta \\ & +\frac{16(2+3q)C_{44}^2}{C_{12}-C_{44}}\Bigg\}. \end{aligned} \tag{41}$$

Again, we first investigate the variation of the passing band with θ. Equations (38) may be written in the form:

$$\begin{gathered} u_j^{l,m,n} = (-1)^{j+1}\sum_{k=1}^{2}(A_{1k}\cos\theta_{3k}n + A_{2k}\sin\theta_{3k}n)\,e^{i[\theta(l+m)-\omega t]}, \qquad u_3^{l,m,n} = 0, \\ 0 \le \operatorname{Re}\theta_{3k} \le \pi, \qquad 0 \le \theta \le \frac{\pi}{2}, \qquad j = 1,2. \end{gathered} \tag{42}$$

For a fixed value of θ, θ_{3k} are determined by the number of atomic layers and the boundary conditions of the lattice plate. Equation (39) can be written in the form

$$\begin{aligned} \frac{M\omega^2}{a} = \frac{1}{2+3q}\{ & 2[(2+3q)(2C_{11}-C_{12}-C_{44})+4(C_{12}-C_{44}) \\ & -3(2+q)(C_{12}-C_{44})\cos\theta_3]\sin^2\theta \\ & +2[2(2+3q)(C_{12}+C_{44})-3(2+q)(C_{12}-C_{44})](1-\cos\theta_3) \\ & +(2-3q)(C_{12}-C_{44})\sin^2\theta_3\}. \end{aligned} \tag{43}$$

Differentiating this equation with respect to θ_3 we obtain,

$$\begin{aligned} \frac{\partial\omega}{\partial\theta_3} = \frac{a\sin\theta_3}{\omega M(2+3q)}\{ & 3(2+q)(C_{12}-C_{44})\sin^2\theta \\ & +[2(2+3q)(C_{12}+C_{44})-3(2+q)(C_{12}-C_{44})] \\ & +(2-3q)(C_{12}-C_{44})\cos\theta_3\}. \end{aligned} \tag{44}$$

The relative extreme values of ω for $\omega \neq 0$ are at

$$\theta_3 = 0, \qquad \pi \tag{45}$$

and

$$\theta_3 = \arccos\left\{\frac{3(2+q)(C_{12}-C_{44})\cos^2\theta - 2(2+3q)(C_{12}+C_{44})}{(2-3q)(C_{12}-C_{44})}\right\} \equiv \theta_{3m}. \tag{46}$$

A real value of θ_{3m} between 0 and π exists if $C_{44} < C_{12}$, and also if

$$\frac{2(2+3q)(C_{12}+C_{44})}{3(2+q)(C_{12}-C_{44})} - \frac{2-3q}{3(2+q)} \leq \cos^2\theta \leq \frac{2(2+3q)(C_{12}+C_{44})}{3(2+q)(C_{12}-C_{44})} + \frac{2-3q}{3(2+q)}, \tag{47}$$

when $|q| < \frac{2}{3}$, or $-2 < q < -\frac{2}{3}$; and if

$$\frac{2(2+3q)(C_{12}+C_{44})}{3(2+q)(C_{12}-C_{44})} + \frac{2-3q}{3(2+q)} \leq \cos^2\theta \leq \frac{2(2+3q)(C_{12}+C_{44})}{3(2+q)(C_{12}-C_{44})} - \frac{2-3q}{3(2+q)}, \tag{48}$$

when $q > \frac{2}{3}$, or $q < -2$. Since, for the time being, we are interested in real θ, i.e. $0 \leq \cos^2\theta \leq 1$, the condition of equation (47) is satisfied if

$$\frac{C_{12}}{C_{44}} > \frac{3(2+q)}{2-3q} \tag{49}$$

and the condition of equation (48) is satisfied if $2 < 0$ i.e. equation (48) will never be satisfied. In addition, for most materials, equation (49) is also not satisfied. Hence the relative maximum is usually at $\theta_3 = \pi$ and the minimum at $\theta_3 = 0$, and they are given by

$$\begin{aligned}\omega_{\min}\\ \omega_{\max}\end{aligned} = \left[\frac{2a}{M(2+3q)}\right]^{\frac{1}{2}} \{&[(2+3q)(2C_{11}-C_{12}-C_{44})+4(C_{12}-C_{44}) \\ &\mp 3(2+q)(C_{12}-C_{44})]\sin^2\theta \\ &+(1\mp 1)[2(2+3q)(C_{12}+C_{44})-3(2+q)(C_{12}-C_{44})]\}^{\frac{1}{2}}. \end{aligned} \tag{50}$$

At $\theta = 0$, the width of the passing band is simply

$$\omega_{\max}(0) - \omega_{\min}(0) = 2\left(\frac{a}{M}\right)^{\frac{1}{2}}\left[2(C_{12}+C_{44}) - \frac{3(2+q)(C_{12}-C_{44})}{2+3q}\right]^{\frac{1}{2}}. \tag{51}$$

At $\theta = \pi/2$

$$\omega_{\max}\left(\frac{\pi}{2}\right) - \omega_{\min}\left(\frac{\pi}{2}\right) = 2\left(\frac{a}{m}\right)^{\frac{1}{2}}[(C_{11}+C_{12}+2C_{44})^{\frac{1}{2}} - (C_{11}-C_{12})^{\frac{1}{2}}]. \tag{52}$$

Just as in the [100] direction, the dispersion relation equation (39) or (43) reduces to a linear equation in $\cos\theta_3$ if either $q = \frac{2}{3}$ or $\gamma_1 = \gamma_2 = 0$. In these cases there is only one wave number in the direction of the thickness of the plate. Nevertheless, the width of the passing band does not reduce to zero in either case. Instead, the dispersion relation, equation (43), reduces to the form:
for $q = \frac{2}{3}$,

$$\cos\theta_3 = 1 + \frac{(C_{11}-C_{12})\sin^2\theta - \dfrac{M\omega^2}{4a}}{2C_{44}+(C_{12}-C_{44})\sin^2\theta}, \tag{53}$$

and for $\gamma_1 = \gamma_2 = 0$,

$$\cos\theta_3 = 1+\frac{1}{2}\left(\frac{C_{11}}{C_{12}}-1\right)\sin^2\theta-\frac{M\omega^2}{8aC_{12}}. \tag{54}$$

Both of these equations give a finite width of the passing band.

We also observe that the central force, next-nearest neighbor interaction has no effect on the *SH*-waves in the [100] direction, but it does in the [110] direction.

When the values of $\cos\theta_{3k}$ obtained from equation (40) are real, the corresponding θ_{3k} are real if $|\cos\theta_{3k}| < 1$ and complex or imaginary if $|\cos\theta_{3k}| > 1$. Furthermore, if

$$\frac{4-9q^2}{C_{12}-C_{44}}\frac{M}{a}(\omega_m^2-\omega^2) < 0, \tag{55}$$

$\cos\theta_{31}$ and $\cos\theta_{32}$ are complex conjugate. Let

$$D_m(\theta) = \frac{4-9q^2}{C_{12}-C_{44}}\frac{M\omega_m^2}{a}. \tag{56}$$

From equation (41), we have

$$D_m(\theta) = P\sin^4\theta+2Q\sin^2\theta+R, \tag{57}$$

where

$$\begin{aligned} P &= 9(2+q)^2, \\ Q &= \frac{2(2+3q)}{C_{12}-C_{44}}[6(2+q)C_{44}+(2-3q)(C_{11}-C_{12})], \\ R &= \left[\frac{4(2+3q)C_{44}}{C_{12}-C_{44}}\right]^2. \end{aligned} \tag{58}$$

We note that in equation (57) P and R are positive definite for all real values of q. Certainly Q is positive for $|q| < \frac{2}{3}$, and $C_{44} < C_{12}$. In the case $|q| > \frac{2}{3}$ and $C_{44} < C_{12} < C_{11}$, Q is positive for almost all known materials. Therefore, $D_m(\theta) > 0$ for $0 \le \theta \le \pi/2$ and equation (57) is positive definite. Thus we conclude that $\cos\theta_{3k}$ in equations (40), will be real in the interval, $0 \le \theta \le \pi/2$ and $\omega^2 < \omega_m^2$ if $|q| < \frac{2}{3}$.

The variation of ω vs. θ_3 is shown in Figs. 8 and 9. We should like to point out that, when the wave number in the propagation direction equals zero, i.e. in the case of thickness modes, the dispersion relations and the boundary conditions are identical in the [100] and [110] directions. In fact, the shear wave with wave normal in the [001] direction, and displacement vector in either [010] or [1$\bar{1}$0] direction has the same dispersion relation, namely,

$$\begin{aligned} \frac{M\omega^2}{a} = \frac{1}{2+3q}\{&(2-3q)(C_{12}-C_{44})\sin^2\theta_3 \\ &+2[2(2+3q)(C_{12}+C_{44})-3(2+q)(C_{12}-C_{44})](1-\cos\theta_3)\}. \end{aligned} \tag{59}$$

The common boundary conditions for $\theta_1 = 0$ or $\theta = 0$ can be obtained by setting $\theta_1 = 0$ in equations (30).

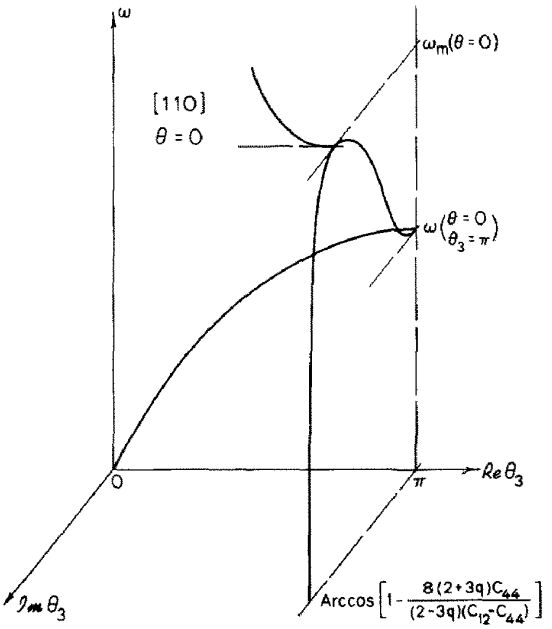

FIG. 8. The variation of ω vs. θ, for SH-waves along the [110] direction, with $\theta = 0$.

We now substitute equations (42) into the boundary conditions, equations (4) and (6), and obtain the system of linear homogeneous equations in A_{jk}:

$$\sum_{k=1}^{2}(F_{jk}A_{1k}\pm G_{jk}A_{2k})=0 \tag{60}$$

where F_{jk} and G_{jk} were defined in equation (31), and

$$\begin{aligned}
f_{1k} &= \frac{a}{2(2+3q)}\{3(2+q)(C_{12}-C_{44})(1+2\cos\theta_{3k})\sin^2\theta \\
&\quad -(2-3q)(C_{12}-C_{44})\sin^2\theta_{3k} \\
&\quad -[4(2+3q)(C_{12}+C_{44})-7(2+q)(C_{12}-C_{44})](1-\cos\theta_{3k})\}, \\
f'_{1k} &= \frac{a\sin\theta_{3k}}{2(2+3q)}\{(C_{12}-C_{44})[(2-3q)\cos\theta_{3k}-6(2+q)\cos^2\theta] \\
&\quad +4(2+3q)(C_{12}+C_{44})+(2+q)(C_{12}-C_{44})\}, \\
f_{2k} &= -\frac{a}{2(2+3q)}(2+q)(C_{12}-C_{44})(1-\cos\theta_{3k}), \\
f'_{2k} &= -\frac{4aq}{2(2+3q)}(C_{12}-C_{44})\sin\theta_{3k}.
\end{aligned} \tag{61}$$

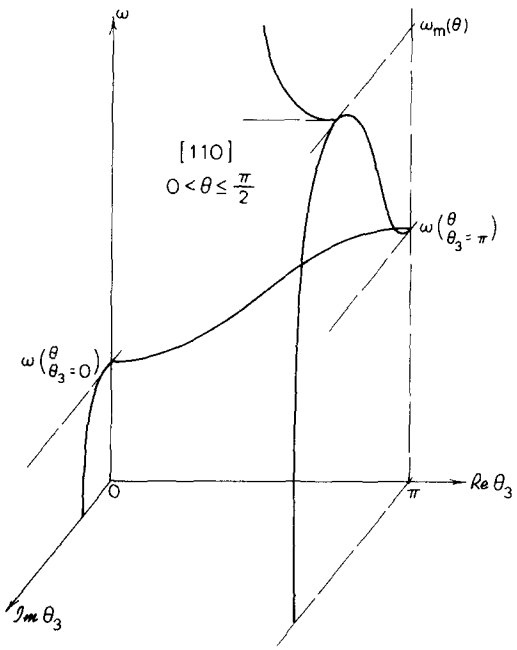

FIG. 9. The variation of ω vs. θ, for SH-waves along the [110] direction, with $0 < \theta \leq \pi/2$.

The condition for a non-trivial solution for A_{jk} yields

$$\|F_{jk}\| = 0 \quad \text{for symmetric modes,} \tag{62a}$$

and

$$\|G_{jk}\| = 0 \quad \text{for antisymmetric modes.} \tag{62b}$$

The amplitude ratio of the two displacement fields associated with the two θ_{3k} is

$$\frac{A_{11}}{A_{12}} = -\frac{H_{12}}{H_{11}} \quad \text{for symmetric modes,} \tag{63a}$$

and

$$\frac{A_{21}}{A_{22}} = -\frac{H_{22}}{H_{21}} \quad \text{for antisymmetric modes,} \tag{63b}$$

where

$$\begin{aligned} H_{1k} &= (2+q)(1-\cos\theta_{3k})\cos\theta_{3k}N - 4q\sin\theta_{3k}\sin\theta_{3k}N, \\ H_{2k} &= (2+q)(1-\cos\theta_{3k})\sin\theta_{3k}N + 4q\sin\theta_{3k}\cos\theta_{3k}N. \end{aligned} \tag{64}$$

NUMERICAL EXAMPLES AND DISCUSSION

There are several differences in the mathematical equations corresponding to waves along the [100] and [110] directions. For waves along the [100] direction only fourth order differences survive in the equations of motion (1). For waves along the [110] direction we get

sixth order differences but of a rather special nature. In both cases the boundary conditions are satisfied, at discrete frequencies, by a superposition of two displacement fields which satisfy the equations of motion at the same frequency. In the [100] direction, the central force interaction between the next nearest neighboring atoms has no influence at all, and in the [110] direction, the effect of this interaction appears only in the equations of motion, i.e. it shows in equation (39). The boundary conditions for both directions are quite similar. The essential differences in dispersion characters arise through equations of motion which yield a substantially different character of dispersion curves and passing bands, as was shown in the preceding section. The frequency equations are transcendental equations which are not easily amenable to analytic investigation. We have therefore carried out numerical computations to obtain the dispersion curves for the plate. We first recall that in the case of an elastic continuum of cubic symmetry, as well as the simple cubic crystal lattice, the relation between the *normalized* frequency and the wave number for face-shear and thickness-twist waves propagating in a transaction-free plate is independent of the elastic constants of the medium [1]. However, in a b.c.c. crystal lattice plate, this relation does depend on the elastic constants: for waves in either the [100] or [110] direction. Therefore, in order to illustrate the changing character of the dispersion relations in different directions, and for different elastic constants, we have considered two different substances. Among the various crystals with reliable experimental data, we have selected iron and tungsten, not only because they are widely used in industry, but also because iron is a crystal strongly deviating from isotropy, whereas tungsten is a crystal very close to isotropy (i.e. for tungsten, $C_{11} \cong C_{12}+2C_{44}$).

Some of the experimental data for iron and tungsten are listed in the following table:

TABLE 1

Name	Units	Iron at 300°K		Tungsten at 295°K	
		Data	Reference	Data	Reference
C_{11}	10^{12} dyn-cm^{-2}	2·331	[8]	5·233825	[11]
C_{12}	10^{12} dyn-cm^{-2}	1·3544	[8]	2·046075	[11]
C_{44}	10^{12} dyn-cm^{-2}	1·1783	[8]	1·607625	[11]
$2a$	Å	2·8606	[9]	3·1650	[9]
M	10^{-23} g	9·2744	[9]	30·548875	[9]
$\hbar\omega_E(\pi)$	meV	35·4	[10]		
$\nu_E(\pi)$	10^{12} c/s			5·50	[12]

Note that the mass, M, calculated for each case is inaccurate, because we cannot obtain the lattice constant, $2a$, and the mass density, ρ, at the same temperature from [9]. However, we use only the ratio of these variables in the present computations. From the given data in the table and using equation (10), we compute the value of q. For iron

$$q = 0{\cdot}53221, \tag{65a}$$

and for tungsten

$$q = -0{\cdot}06982. \tag{65b}$$

Note that

$$\begin{aligned} h(\text{Planck's constant}) &= 6{\cdot}6255 \times 10^{-27}\ \text{ergs-sec}, \\ \hbar = \frac{h}{2\pi} &= 1{\cdot}05456 \times 10^{-27}\ \text{ergs-sec}, \\ 1\ \text{eV} &= 1{\cdot}6019 \times 10^{-12}\ \text{ergs}, \\ \omega_E(\pi) &= \frac{1{\cdot}6019 \times 10^{-15}}{1{\cdot}05456 \times 10^{-27}}[\hbar\omega_E(\pi)] \\ &= 1{\cdot}52 \times 10^{12}\ \text{rad-sec}^{-1}[\hbar\omega_E(\pi)], \\ \omega_E(\pi) &= 2\pi\nu_E(\pi)\ \text{rad-sec}^{-1}. \end{aligned} \tag{66}$$

Just as in the case of a simple cubic crystal lattice plate [1], we also choose the frequency of the first (antisymmetric) thickness-shear (i.e. $\theta_1 = 0$, or $\theta = 0$) mode as the reference frequency:

$$\omega_1 = \frac{2\pi}{2N+1}\left(\frac{aC_{44}}{M}\right)^{\frac{1}{2}} = \frac{\pi}{a(2N+1)}\left(\frac{C_{44}}{\rho}\right)^{\frac{1}{2}}, \tag{67}$$

thus the normalized frequency is

$$\Omega = \frac{\omega}{\omega_1}. \tag{68}$$

In this paper we restrict our discussion to the real branches of the dispersion curves; i.e. in the $\Omega - \theta_1$ (or $\Omega - \theta$) relation, only real θ_1 (or real θ) has been considered.

The dispersion curves for real wave-number with face-shear and thickness-twist waves propagating in the [100] and [110] directions of a b.c.c. crystal lattice plate 15 atomic layers thick are shown in Figs. 10 and 12, for iron, and in Figs. 11 and 13 for tungsten. In these figures one may see that the pattern of the dispersion curves in a plate is strongly influenced by the shape of the passing band found in the unbounded lattice. In particular, for *SH*-waves in the [100] direction, the real branches are squeezed closely together at $\theta_1 = \pi/2$, for iron as well as tungsten. From equation (24), we find the passing band at $\theta_1 = \pi/2$

$$\omega\left(\frac{\pi}{2}\right) - \omega(0) = 0{\cdot}00104814\left(\frac{8aC_{44}}{M}\right)^{\frac{1}{2}}, \text{for iron}, \tag{69}$$

$$\omega\left(\frac{\pi}{2}\right) - \omega(0) = 0{\cdot}02125976\left(\frac{8aC_{44}}{M}\right)^{\frac{1}{2}}, \text{for tungsten}. \tag{70}$$

For waves propagating in the [110] direction, $\theta = \pi/2$ is the boundary of the first Brillouin zone, and the dispersion curves for propagating waves must be terminated at that point. In the [100] direction, the first Brillouin zone is ended at $\theta_1 = \pi$, however, the dispersion curves for the lattice plate with an odd number of atomic layers across the thickness are symmetric about $\theta_1 = \pi/2$, even though the dispersion relation, equation (12), for the unbounded b.c.c. crystal lattice is asymmetric. It may be shown that the dispersion curves for a plate with an even number of atomic layers across the thickness are not symmetric about $\theta_1 = \pi/2$. Rather, the dispersion curves of the symmetric and antisymmetic modes

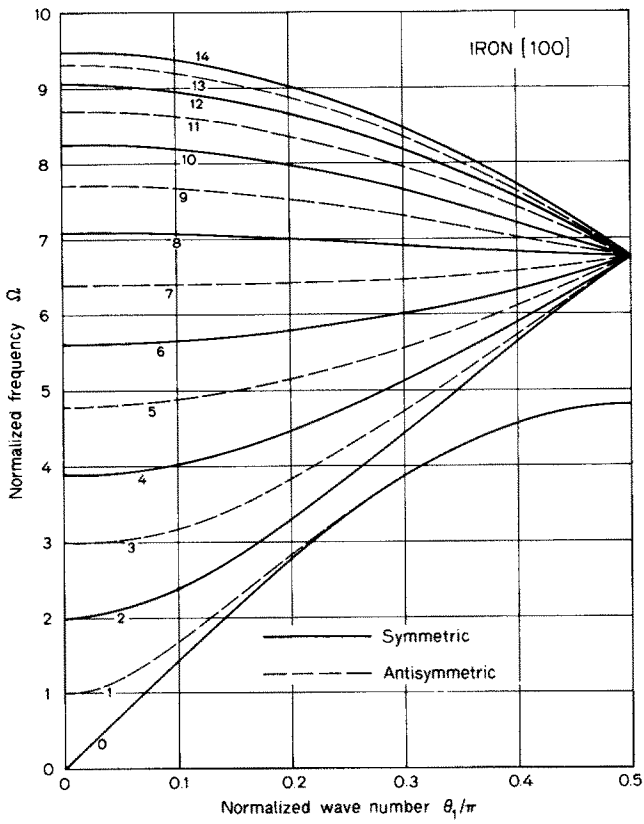

FIG. 10. Real branches of the dispersion relation for face-shear and thickness-twist waves along the [100] direction in a plate 15 atomic layers thick (iron).

are mirror images of each other across the line $\theta_1 = \pi/2$. In our present computations, because of the symmetry, we give only the portion, from $\theta_1 = 0$ to $\theta_1 = \pi/2$, of the real branches of the dispersion curves for the plate with fifteen atomic layers, in Figs. 10 and 11. As we have already noted, in either the [100] or [110] direction, the characteristic values of θ_{3k} are functions of the wave number in the direction of propagation. Consequently, the mode shapes of the thickness-shear vibrations ($\theta_1 = 0$, or $\theta = 0$) cannot be maintained invariant along each branch as the wavelength diminishes from the infinity. This is in contrast with the case of the continuum theory as well as the simple cubic crystal lattice theory [1], where the mode shapes of the thickness-shear do not vary as the value of the wave number of the thickness-twist waves propagating in a principal direction changes.

In the [100] direction, the spectrum of the real branches has three regions which are distinguished by the characters of θ_{3k}, i.e. in the first region one of the $\theta_{3k}(\theta_{31}$, for iron and tungsten) is imaginary and the other is complex (for iron and tungsten the real part of this wave number is always equal to π). The second region has one of θ_{3k} (θ_{31} in our examples) real and the other complex (with real part equal to π), and the third region has both θ_{3k} real. The first region contains only two branches, i.e. the first branch of the symmetric modes and

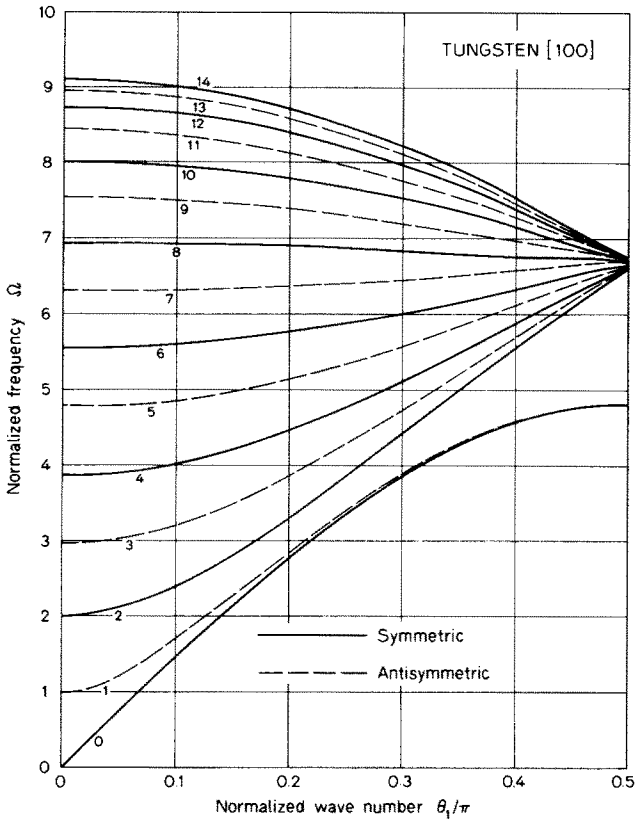

FIG. 11. Real branches of the dispersion relation for face-shear and thickness-twist waves along the [100] direction in a plate 15 atomic layers thick (tungsten).

a part of the first branch of the antisymmetric modes. As $\theta_1 \to 0$, both branches approach bulk modes analogous to the extensional and flexural modes of a continuum plate. The same two branches nearly merge into one as θ_1 approaches $\pi/2$. The mode shape of the first symmetric branch then consists of two kinds of surface-like modes, i.e.

$$u^{l,m,n}_{2(0)} = B_{11}\left[\cosh n\theta_{31(0)} + \frac{B_{12}}{B_{11}}(-1)^n \cosh n\theta_{32(0)}\right] e^{i(\theta_1 l - \omega t)}, \tag{71}$$

where $\theta_{3k(0)}$ designates the imaginary part of θ_{3k} of the first symmetric branch. The first term in equation (71) is a monotonic decay surface-like mode, and the second term is an alternating decay surface-like mode. The ratio B_{12}/B_{11} is very small when θ_1 is small, when also $\theta_{31(0)}$ is quite small as compared to $\theta_{32(0)}$. As θ_1 and the frequency increase, $\theta_{31(0)}$ approaches $\theta_{32(0)}$ and the ratio B_{12}/B_{11} approaches $(-1)^N$. At $\theta_1 = \pi/2$, we find $\theta_{31(0)} = \theta_{32(0)}$ and $B_{12}/B_{11} = (-1)^N$, and equation (71) reduces to

$$u^{l,m,n}_{2(0)}\left(\theta_1 = \frac{\pi}{2}\right) = B_{11}[1 + (-1)^{N+n}] \cosh n\theta_{31(0)}\, e^{i(\pi l/2 - \omega t)}. \tag{72}$$

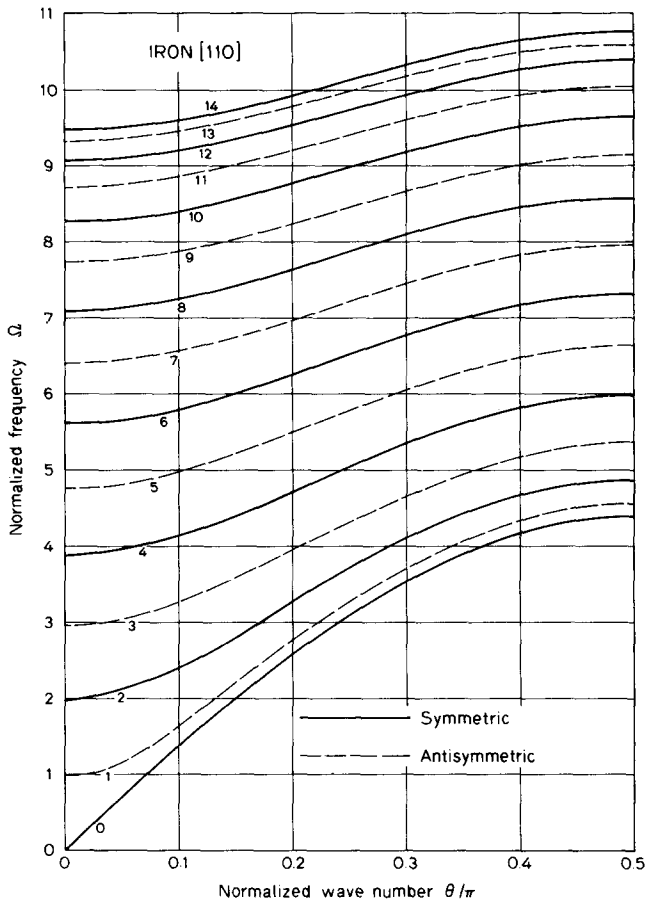

FIG. 12. Real branches of the dispersion relation for face-shear and thickness-twist waves along the [110] direction in a plate 15 atomic layers thick (iron).

It is seen that at $\theta_1 = \pi/2$, the amplitude of the motion of the atoms is zero if they are on the layer with $N+n$ odd, and doubled if $N+n$ even.

The first antisymmetric mode branch starts, at $\theta_1 = 0$, as a bulk mode. At the point of inflection of the dispersion curve the character of this mode changes into that of a surface-like mode. As in the case of the lower symmetric mode, the antisymmetric surface-like mode is a superposition of two displacement fields, one monotonic and one of alternating sign, both decreasing exponentially in magnitude away from the surfaces of the plate.

The existence of a surface mode, associated with shear displacements only, is of particular interest. This mode differs from previous structural surface modes in lattices which were of the Rayleigh or generalized-Rayleigh type and involved coupled longitudinal and shear waves [13]. In the present case, the displacements are linearly polarized in a direction normal to the direction of propagation and parallel to the free surfaces. It may be pointed out that the possibility of existence of surface modes other than of the Rayleigh type has been suggested by Feuchtwang [4], and confirmed previously by Allen *et al.* [5].

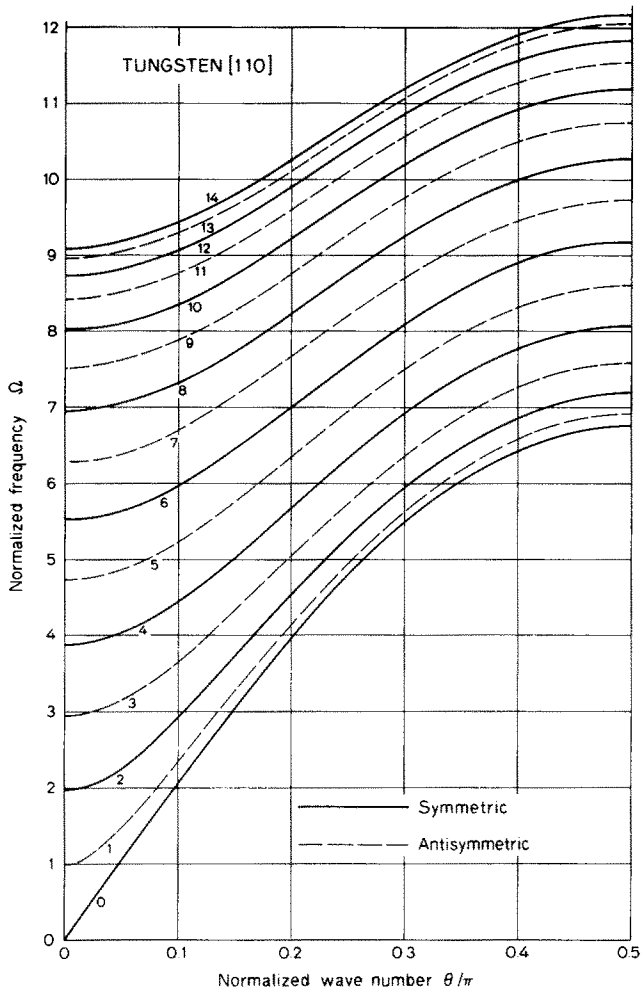

FIG. 13. Real branches of the dispersion relation for face-shear and thickness-twist waves along the [110] direction in a plate 15 atomic layers thick (tungsten).

All modes in the second region are essentially bulk modes. The mode shapes across the thickness of the plate are dominated by the sinusoidal contribution associated with the real θ_{31}, but in the vicinity of the plate surfaces the mode shapes are influenced by the surface component associated with the complex θ_{32}. As an example we have computed the amplitude ratio and the θ_{3k} for each branch at certain fixed values of θ_1 for tungsten (see Table 6).

Among the fifteen branches, except for the first one which has zero curvature at $\Omega = 0$, we find that the first seven branches have positive curvatures at the cut-off frequencies (i.e. at $\theta_1 = 0$), therefore, along each of them the velocity of energy propagation (or group velocity) is positive if $0 < \theta_1 < \theta_A$, where $0 < \theta_A < \pi/2$ is the boundary of the second region for each branch. The remaining seven branches have negative curvatures at $\theta_1 = 0$, and along each of them the group velocity is negative for $0 < \theta_1 < \theta_A$. Besides the evident

TABLE 2. THE DISPERSION RELATION (Ω VS. θ_1/π) FOR FACE-SHEAR AND THICKNESS-TWIST WAVES IN THE [100] DIRECTION IN A PLATE 15 ATOMIC LAYERS THICK (IRON)

Mode	θ_1/π					
	0	0·10	0·20	0·30	0·40	0·50
0	0·0	1·438962	2·790347	3·877147	4·565716	4·803458
1	0·998219	1·696123	2·845076	3·878797	4·565717	4·803458
2	1·985754	2·388893	3·304413	4·449235	5·645150	6·745646
3	2·951927	3·203403	3·851178	4·736409	5·749205	6·746628
4	3·886114	4·044567	4·480411	5·120748	5·908868	6·745746
5	4·777843	4·871494	5·139529	5·557135	6·108782	6·746994
6	5·616957	5·661716	5·794199	6·014180	6·333434	6·748048
7	6·393822	6·399906	6·420979	6·468239	6·568577	6·749623
8	7·099550	7·074276	7·002955	6·901108	6·801748	6·748733
9	7·726210	7·675304	7·527420	7·298693	7·022396	6·750523
10	8·266996	8·195270	7·984660	7·650128	7·221868	6·751041
11	8·716323	8·628046	8·367288	7·947155	7·393301	6·752022
12	9·069855	8·968959	8·669831	8·183676	7·531472	6·751870
13	9·324434	9·214645	8·888417	8·355385	7·632620	†
14	9·477965	9·362885	9·020510	8·459460	7·694248	†

† The values of Ω are very close to 6·752.

mathematical reasons, we would like to give a physical explanation for the existence of both positive and negative group velocities along the real branches: in the equilibrium position, the atoms on every next layer of the b.c.c. crystal lattice are displaced by a vector distance $\mathbf{v} = a(\pm\mathbf{e}_1 \pm \mathbf{e}_2)$. In the [100] direction, the positions of atoms between adjacent layers, therefore, have a spatial phase difference a, which for waves propagating in the [100] direction, marks the phase difference between adjacent layers. Accordingly, across the

TABLE 3. THE DISPERSION RELATION (Ω VS. θ_1/π) FOR FACE-SHEAR AND THICKNESS-TWIST WAVES IN THE [100] DIRECTION IN A PLATE 15 ATOMIC LAYERS THICK (TUNGSTEN)

Mode	θ_1/π					
	0·0	0·10	0·20	0·30	0·40	0·50
0	0·0	1·440397	2·790270	3·880329	4·571981	4·810910
1	0·997803	1·700074	2·840055	3·882888	4·571984	4·810910
2	1·982474	2·390800	3·305687	4·423425	5·574129	6·615712*
3	2·941121	3·199355	3·854433	4·725380	5·696075	6·634993
4	3·861358	4·028147	4·478689	5·118902	5·877011	†
5	4·731593	4·835024	5·124273	5·555558	6·094373	6·636368
6	5·541340	5·597121	5·756280	6·002359	6·327559	6·662770
7	6·281495	6·299620	6·351745	6·435525	6·559657	6·693505
8	6·944571	6·932130	6·895209	6·838082	6·777811	6·665430
9	7·524824	7·487336	7·376283	7·198322	6·973053	6·697364
10	8·018261	7·960363	7·788255	7·508638	7·139867	6·721206
11	8·422503	8·348329	8·127158	7·764567	7·275566	6·740820
12	8·736529	8·649912	8·391033	7·963935	7·379550	6·725854
13	8·960277	8·864874	8·579270	8·106076	7·452499	6·745419
14	9·094188	8·993553	8·691989	8·191122	7·495586	6·750226

† The value of Ω at this point is very close to that at *.

TABLE 4. THE DISPERSION RELATION (Ω VS. θ/π) FOR FACE-SHEAR AND THICKNESS-TWIST WAVES IN THE [110] DIRECTION IN A PLATE 15 ATOMIC LAYERS THICK (IRON)

Mode	θ/π					
	0·0	0·10	0·20	0·30	0·40	0·50
0	0·0	1·355689	2·577383	3·545539	4·166423	4·380240
1	0·998219	1·695689	2·790561	3·720943	4·328629	4·539096
2	1·985754	2·417193	3·288797	4·118574	4·683329	4·881779
3	2·951927	3·262788	3·962990	4·686346	5·198557	5·381374
4	3·886114	4·132428	4·716980	5·352359	5·816041	5·983721
5	4·777843	4·985494	5·492266	6·060711	6·484452	6·639221
6	4·616957	5·799719	6·253102	6·771965	7·164484	7·308894
7	6·393822	6·559796	6·975765	7·458153	7·826846	7·963206
8	7·099550	7·253858	7·643194	8·098779	8·449523	8·579739
9	7·726210	7·872269	8·242471	8·678391	9·015738	9·141329
10	8·266996	8·407179	8·763616	9·185184	9·512642	9·634798
11	8·716323	8·852345	9·198961	9·610195	9·930477	10·050129
12	9·069855	9·202994	9·542780	9·946780	10·262014	10·379902
13	9·324434	9·455689	9·790993	10·190231	10·502131	10·618851
14	9·477965	9·608153	9·940921	10·337455	10·647459	10·763514

thickness of the plate, there are two groups of atoms, and in each of these groups the atoms have the same spatial phase in the [100] direction. Upon drawing an analogy to the one dimensional diatomic lattice with identical masses but different force constant [14], we find that when the mass centers of the two groups of atoms move accordantly during the wave motion, we have motion analogous to the acoustic mode. The optical modes correspond to the wave motions during which the mass centers of the two groups of atoms move oppositely. In Figs. 14 and 15, we give the typical mode shapes across the thickness of the plate of tungsten at $\theta_1 = 0$ and $\theta_1 = 0{\cdot}2\pi$ respectively. Note that Fig. 14 is also valid for the [110] direction, because, as we have shown, the thickness-shear modes in both [100] and [110]

TABLE 5. THE DISPERSION RELATION (Ω VS. θ/π) FOR FACE-SHEAR AND THICKNESS-TWIST WAVES IN THE [110] DIRECTION IN A PLATE 15 ATOMIC LAYERS THICK (TUNGSTEN)

Mode	θ/π					
	0·0	0·10	0·20	0·30	0·40	0·50
0	0·0	2·099259	3·987579	5·481865	6·439754	6·769624
1	0·997803	2·348783	4·159579	5·638243	6·592686	6·921984
2	1·982474	2·917705	4·528365	5·941907	6·874242	7·198156
3	2·941121	3·650194	5·056608	6·380576	7·277304	7·591808
4	3·861358	4·438977	5·680714	6·915379	7·772602	8·076125
5	4·731593	5·227666	6·346488	7·503902	8·324202	8·617099
6	5·541340	5·984336	7·013831	8·109196	8·898153	9·181813
7	6·281495	6·688823	7·654060	8·701723	9·465663	9·741836
8	6·944571	7·327461	8·246758	9·258829	10·003669	10·274078
9	7·524824	7·890816	8·777500	9·763653	10·494427	10·760585
10	8·018261	8·372564	9·236341	10·204055	10·924807	11·187949
11	8·422503	8·768799	9·616758	10·571694	11·285547	11·546631
12	8·736529	9·077469	9·914819	10·861209	11·570504	11·830246
13	8·960277	9·297825	10·128457	11·069469	11·775937	12·034859
14	9·094188	9·429866	10·256798	11·194868	11·899810	12·158295

TABLE 6. THE AMPLITUDE RATIOS $B_{k1}/B_{k2}(B_{11}/B_{12}$ FOR SYMMETRIC MODES, B_{21}/B_{22} FOR ANTISYMMETRIC MODES) AND THE WAVE NUMBERS θ_{3k} (IN RAD.) IN THE [001] DIRECTION (NORMAL TO THE PLANE OF THE PLATE) FOR FACE-SHEAR AND THICKNESS-TWIST WAVES PROPAGATING ALONG THE [100] DIRECTION IN A PLATE 15 ATOMIC LAYERS THICK (TUNGSTEN)

Mode	$\theta_1/\pi = 0{\cdot}0$			$\theta_1/\pi = 0{\cdot}20$		
	θ_{31}	$\theta_{32}-\pi$	$B_{k1}/B_{k2}(10^{12})$	θ_{31}	$\theta_{32}-\pi$	$B_{k1}/B_{k2}(10^{12})$
0	0·0	3·861183i	∞	0·212333i	3·617520i	−1·960762
1	0·209458	3·817204i	292·453674	0·165223i	3·617039i	−3·271763
2	0·419025	3·814355i	−73·370691	0·351249	3·613013i	8·030406
3	0·628788	3·809722i	−32·833467	0·585794	3·607292i	15·416054
4	0·838797	3·803479i	18·688476	0·807149	3·599569i	29·036831
5	1·049053	3·795868i	12·193903	1·024108	3·590130i	6·074632
6	1·259505	3·787196i	−8·729651	1·239113	3·579345i	−3·123137
7	1·470050	3·777825i	−6·719141	1·453069	3·567654i	−2·031152
8	1·680542	3·768162i	5·513671	1·666320	3·555558i	1·501076
9	1·890809	3·758641i	4·819783	1·878962	3·543598i	1·220308
10	2·100678	3·749696i	−4·513168	2·090980	3·532324i	−1·083220
11	2·310000	3·741743i	−4·585881	2·302322	3·522268i	−1·057280
12	2·518690	3·735150i	5·186265	2·512964	3·513907i	1·160570
13	2·726755	3·730218i	6·900399	2·722948	3·507640i	1·512451
14	2·934315	3·727170i	−12·829519	2·932414	3·503759i	−2·777613

directions are identical. We note that all modes above the seventh tend to have a displacement variation across the thickness characteristic of an optical mode.

In a graph of small scale, we cannot see the influence of the surface components of the displacement. In order to show the effect of this surface component on the sinusoidal modes, we have tabulated the normalized displacements through the thickness for both $\theta_1 = 0$ and $\theta_1 = 0{\cdot}2\pi$. As the numerical results (for tungsten, for example) show that the surface components of the displacements hardly have any influence on the layers with $0 \leq n \leq 3$, we give only the total normalized displacements for these layers in Tables 7 and 9. In Tables 8 and 10, we give the normalized displacements both with and without the contribution of the surface component of the displacement, for $4 \leq n \leq 7$. In Tables 9 and 10, the surface-like modes are also included. For most materials the third region of the spectrum is very small. The size of the region is directly related to the width of the passing band in the vicinity of $\theta_1 = \pi/2$. In Fig. 10 or 11, this region is so small that the intricate behavior of the branches is not visible; hence in Fig. 16 we have drawn an enlarged detail of the third region for tungsten. In this region both θ_{3k} are real and they correspond to two superimposed sinusoidal modes through the thickness of the plate, for each value of θ_1. As θ_1 approaches $\pi/2$, more branches enter the third region. In the second region the mode shapes through the thickness of the plate are dominated by the mode shapes for a single, real θ_{3k} (in the present examples it is θ_{31}).

In the third region, where both θ_{3k} are real, the fluctuation of the amplitude ratios, (B_{k1}/B_{k2}), is of the order $\pm 10^{\pm 3}$ for tungsten. Instead of being monotonic, as in the second region, the branches are wavy and the group of branches of symmetric modes intersects with that of the antisymmetric modes. Thus at a certain frequency and a certain wave number θ_1, there may simultaneously exist one symmetric and one antisymmetric mode in the plate. The fluctuation of the amplitude ratios (B_{k1}/B_{k2}) is closely related to the curvature and slope along each branch: $B_{k1}/B_{k2}(k = 1$ or $2)$ attains a maximum at the point where the group

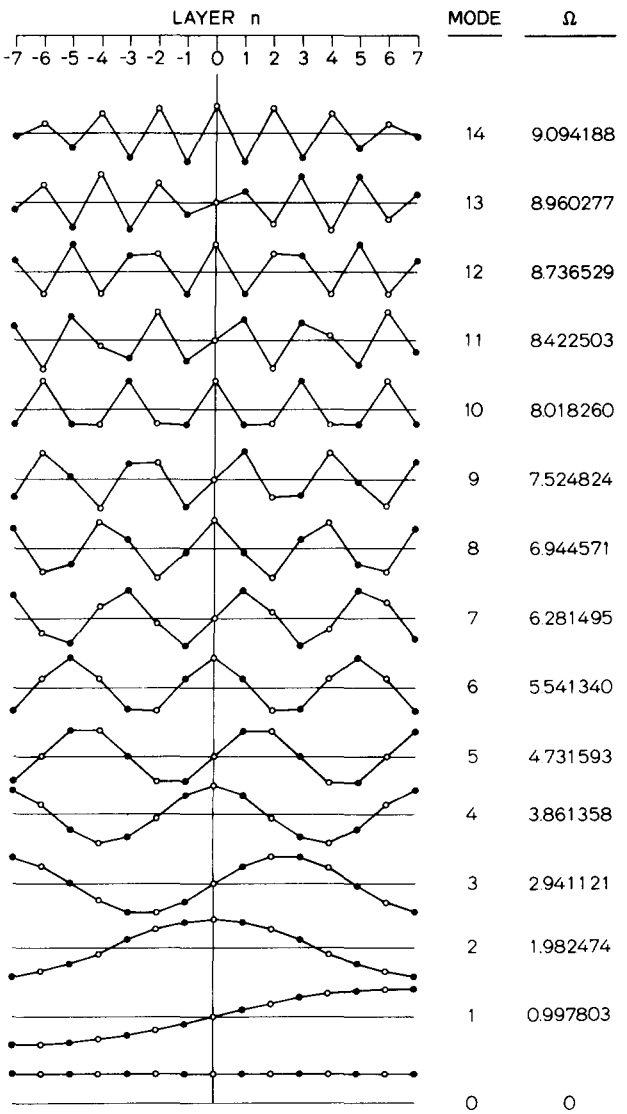

FIG. 14. Mode shapes and normalized frequencies of thickness-shear vibrations in either the [010] direction (i.e. face-shear and thickness-twist waves along the [100] direction with $\theta_1 = 0$) or the [1$\bar{1}$0] direction (i.e. face-shear and thickness-twist waves along the [110] direction with $\theta = 0$) of a plate 15 atomic layers thick (tungsten). Note that in a (010) plane of the plate, the atoms of adjacent layers are not in phase along the [100] direction in the equilibrium position. In this figure, however, we have eliminated the phase difference for convenience and have used "white circle" and "black circle" to indicate the difference.

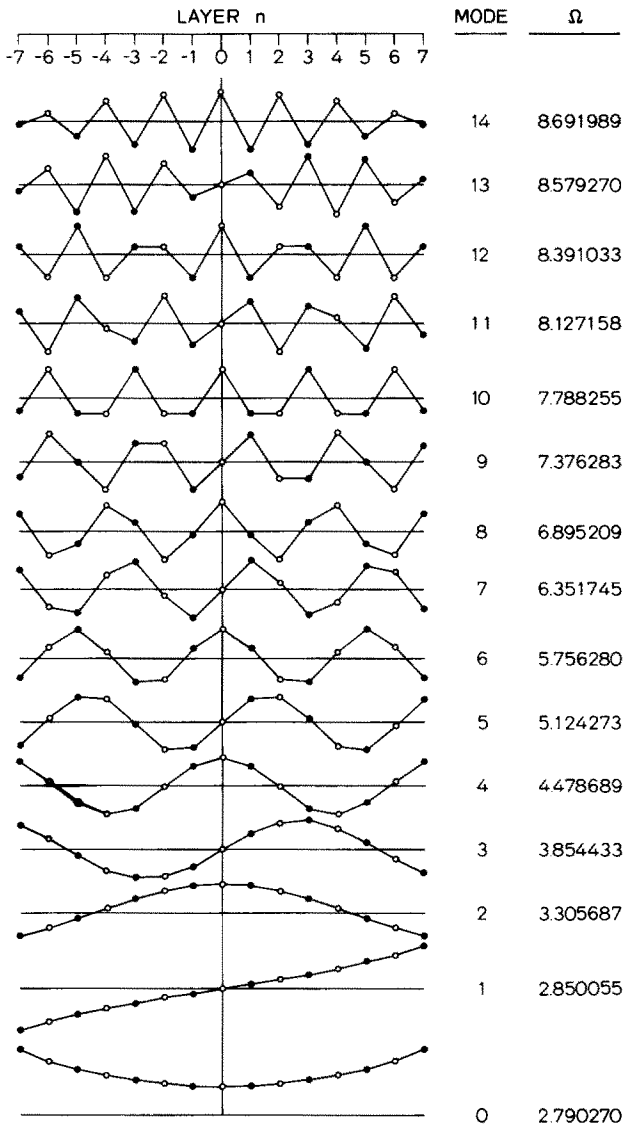

FIG. 15. Mode shapes and normalized frequencies of face-shear and thickness-twist waves along the [100] direction with $\theta_1 = \pm 0{\cdot}2\pi$ in a plate 15 atomic layers thick (tungsten). Note that in a (010) plane of the plate, the atoms of adjacent layers are not in phase along the [100] direction in the equilibrium position. In this figure, however, we have eliminated the phase difference for convenience and have used "white circle" and "black circle" to indicate the difference.

TABLE 7. THE NORMALIZED DISPLACEMENTS OF THE LAYERS WITH $0 \leq n \leq 3$, (UPON WHICH THE SURFACE COMPONENTS OF THE DISPLACEMENTS HAVE NEGLIGIBLE INFLUENCE) FOR THE THICKNESS-SHEAR VIBRATIONS IN EITHER THE [010] DIRECTION (i.e. FACE-SHEAR AND THICKNESS-TWIST WAVES ALONG THE [100] DIRECTION WITH $\theta_1 = 0$) OR THE [1$\bar{1}$0] DIRECTION (i.e. FACE-SHEAR AND THICKNESS-TWIST WAVES ALONG THE [110] DIRECTION WITH $\theta = 0$) IN A PLATE 15 ATOMIC LAYERS THICK (TUNGSTEN)

Mode	Layer n			
	0	1	2	3
0	1·00	1·00	1·00	1·00
1	0·00	0·20792997	0·40677078	0·58783060
2	1·00	0·91348616	0·66891394	0·30860110
3	0·00	0·58816460	0·95134594	0·95062081
4	1·00	0·66835847	−0·10659390	−0·81084435
5	0·00	0·86695170	0·86416386	−0·00556673
6	1·00	0·30628791	−0·81237544	−0·80392945
7	0·00	0·99492936	0·20013232	−0·95467228
8	1·00	−0·10952502	−0·97600854	0·32331971
9	0·00	0·94923143	−0·59721579	−0·57348881
10	1·00	−0·50543099	−0·48907903	0·99982239
11	0·00	0·73900558	−0·99573509	0·60264651
12	1·00	−0·81218819	0·31929932	0·29352591
13	0·00	0·40304154	−0·73771247	0·94724034
14	1·00	−0·97859483	0·91529569	−0·81281242

velocity is a maximum, and a minimum at minimum group velocity. The ratio B_{k1}/B_{k2} equals unity at the point of zero group velocity. The sign of the amplitude ratio depends on the curvature of the branch as well as the number of layers of the plate, and the order of the branch. At $\theta_1 = \pi/2$, we find

$$\frac{B_{11}}{B_{12}} = (-1)^N, \qquad \frac{B_{21}}{B_{22}} = (-1)^{N+1}, \tag{73}$$

and $\theta_{31} + \theta_{32} = \pi$. Thus, from equation (15), we obtain

$$u_2^{l,m,n} = [1 + (-1)^{N+n}](B_{11} \cos \theta_{31} n + B_{21} \sin \theta_{31} n)\, e^{i[(\pi l/2) - \omega t]}. \tag{74}$$

The pattern of the branches shown in Fig. 16 implies the existence of two systems of bounding curves which intersect one another in the third region. Through every other intersection point there passes one branch of a symmetric mode and one branch of an antisymmetric mode. It is instructive to recall the case of extensional and flexural waves in a continuum plate where analogous bounds have been found by Mindlin [15] to be branches of the dispersion curves of a plate with mixed boundary conditions.

Since the width of the passing band is fixed for fixed material constants, and for every value of θ_1, an increase of the number of atomic layers across the thickness of the plate

TABLE 8. THE NORMALIZED DISPLACEMENTS OF THE LAYERS WITH $4 \leq n \leq 7$, (A) WITH AND (B) WITHOUT THE CONTRIBUTION OF THE SURFACE COMPONENT OF THE DISPLACEMENT. THE THICKNESS-SHEAR VIBRATIONS ARE IN EITHER THE [010] DIRECTION (i.e. FACE-SHEAR AND THICKNESS-TWIST WAVES ALONG THE [100] DIRECTION WITH $\theta_1 = 0$) OR THE [1$\bar{1}$0] DIRECTION (i.e. FACE-SHEAR AND THICKNESS-TWIST WAVES ALONG THE [110] DIRECTION WITH $\theta = 0$) IN A PLATE 15 ATOMIC LAYERS THICK (TUNGSTEN)

Mode		Layer n			
		4	5	6	7
0		1·00	1·00	1·00	1·00
1	*A*	0·74319484	0·86607178	0·95110628	0·99384778
	B	0·74319483	0·86607211	0·95190115	0·99453556
2	*A*	−0·10510830	−0·50062969	−0·80958998	−0·97567190
	B	−0·10510827	−0·50063100	−0·80953027	−0·97835922
3	*A*	0·58626651	−0·00234203	−0·59018818	−0·94625229
	B	0·58626658	−0·00234489	−0·59005939	−0·95206584
4	*A*	−0·97727537	−0·49550120	0·31515508	0·90670111
	B	−0·97727548	−0·49549634	0·31493712	0·91647813
5	*A*	−0·86971252	−0·86135640	0·01145241	0·85823978
	B	−0·86971268	−0·86134924	0·01113328	0·87244671
6	*A*	0·31990748	0·99990676	0·29218194	−0·80197847
	B	0·31990770	0·99989717	0·29260512	−0·82065435
7	*A*	−0·39216711	0·87579892	0·56781367	−0·73874194
	B	−0·39216684	0·87578703	0·56833341	−0·76146546
8	*A*	0·90518567	−0·52161440	−0·79033102	0·66897301
	B	0·90518535	−0·52160060	−0·79092872	0·69485356
9	*A*	0·95803076	−0·02927799	−0·93897365	0·59273375
	B	0·95803041	−0·02926293	−0·93961942	0·62043127
10	*A*	−0·52160376	−0·47253797	0·99863599	−0·50980648
	B	−0·52160340	−0·47255334	0·99928960	−0·53759052
11	*A*	0·18372969	−0·85018955	0·96122050	−0·41990654
	B	0·18373003	−0·85020409	0·96183378	−0·44576941
12	*A*	−0·79609559	0·99962100	−0·82716382	0·32300126
	B	−0·79609589	0·99963344	−0·82768507	0·34483865
13	*A*	−0·99608134	0·87594173	−0·60684646	0·21963903
	B	−0·99608156	0·87595086	−0·60722680	0·23549484
14	*A*	0·67553227	−0·50932775	0·32112721	−0·11121937
	B	0·67553239	−0·50933258	0·32132807	−0·11956740

simply increases the number of branches within the fixed passing band. Concomitantly, the normalized frequency at cut-off ($\theta_1 = 0$) of the lowest branch of the antisymmetric modes approaches unity from below and the cut-off frequencies of first few immediately higher branches are nearly integer numbers. For the branches of the higher modes, however, the deviation from equal spacing of cut-off frequencies is appreciable.

In the [110] direction, the real branches of the dispersion spectrum, though heavily material-dependent (cf. the spectra for iron and tungsten, for example), are quite similar to those for the simple cubic crystal lattice [1]. Along each real branch the mode shapes of the plate, varying slightly with the wave number θ in the direction of propagation, consist of a superposition of one sinusoidal component due to the real θ_{3k} (θ_{31} in the present examples) and one surface component due to the complex θ_{3k} with real part equal to π. The influence of the surface component is insignificant. The amplitude ratios A_{k1}/A_{k2}

TABLE 9. THE NORMALIZED DISPLACEMENTS OF THE LAYERS WITH $0 \leq n \leq 3$, (UPON WHICH THE SURFACE COMPONENTS OF THE DISPLACEMENTS HAVE NEGLIGIBLE INFLUENCE) FOR THE FACE-SHEAR AND THICKNESS-TWIST WAVES PROPAGATING IN THE [100] DIRECTION, WITH $\theta_1 = 0{\cdot}2\pi$ IN A PLATE 15 ATOMIC LAYERS THICK (TUNGSTEN)

Mode	Layer n			
	0	1	2	3
0	1·00	1·02262752	1·09153410	1·20983801
1	0·00	0·1659761	0·33649353	0·51621771
2	1·00	0·93894379	0·76323089	0·49431802
3	0·00	0·55286093	0·92136877	0·98264350
4	1·00	0·69156050	−0·04348814	−0·75170987
5	0·00	0·85425075	0·88818363	0·06921365
6	1·00	0·32563466	−0·78792414	−0·83878546
7	0·00	0·99307817	0·23328466	−0·93827710
8	1·00	−0·09537839	−0·98180592	0·28266451
9	0·00	0·95289151	−0·57804559	−0·60223598
10	1·00	−0·49703931	−0·50590384	0·99994753
11	0·00	0·74415584	−0·99420121	0·58410901
12	1·00	−0·80883477	0·30842738	0·30990118
13	0·00	0·40652233	−0·74283081	0·95083880
14	1·00	−0·97820186	0·91375777	−0·80947724

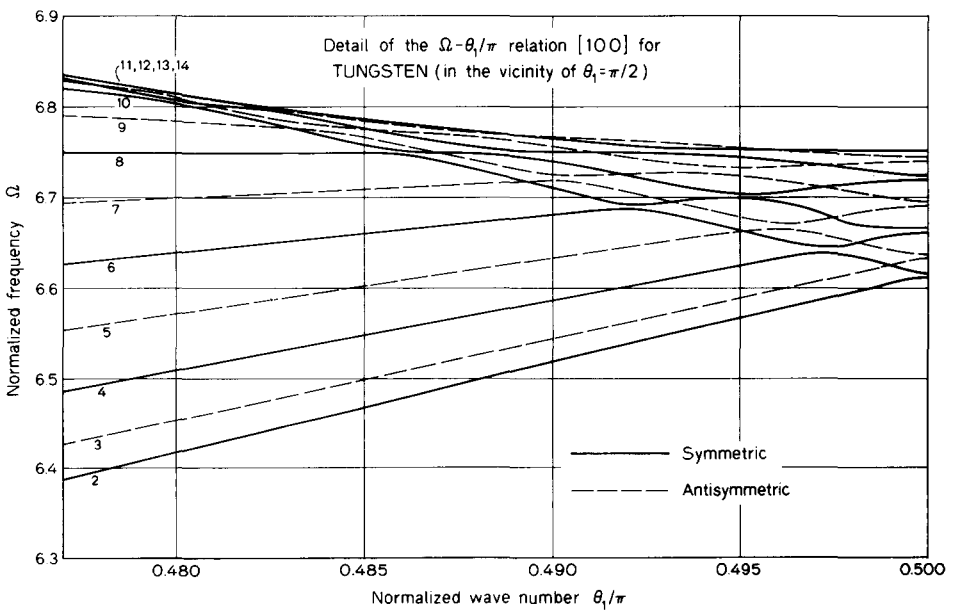

FIG. 16. Enlarged detail of the real branches in the passing band near $\theta_1 = \pi/2$ of the dispersion relation for thickness-twist waves along the [100] direction in a plate 15 atomic layers thick (tungsten).

TABLE 10. THE NORMALIZED DISPLACEMENTS OF THE LAYERS WITH $4 \leq n \leq 7$, (A) WITH AND (B) WITHOUT THE CONTRIBUTION OF THE SURFACE COMPONENT OF THE DISPLACEMENT. THE FACE-SHEAR AND THICKNESS-TWIST WAVES ARE PROPAGATING IN THE [100] DIRECTION WITH $\theta_1 = 0{\cdot}2\pi$ IN A PLATE 15 ATOMIC LAYERS THICK (TUNGSTEN)

Mode		Layer n			
		4	5	6	7
0		1·38289281	1·61854968	1·92673550	2·34887917
1		0·71006577	0·92335342	1·16147563	1·44735537
2	*A*	0·16504291	−0·18439058	−0·51113760	−0·78177462
	B	0·16504279	−0·18438621	−0·51129937	−0·77577654
3	*A*	0·71625295	0·21102346	−0·36448726	−0·82159838
	B	0·71625289	0·21102566	−0·36456869	−0·81859654
4	*A*	−0·99621753	−0·62618070	0·13017672	0·80466280
	B	−0·99621756	−0·62617957	0·13013544	0·80617264
5	*A*	−0·81622050	−0·91786167	−0·13790893	0·76752007
	B	−0·81622064	−0·91785653	−0·13809535	0·77427571
6	*A*	0·24164864	0·99617347	0·40678225	−0·71883336
	B	0·24164891	0·99616399	0·40712213	−0·73101784
7	*A*	−0·45369636	0·83171283	0·64858377	−0·66196248
	B	−0·45369597	0·83169908	0·64907097	−0·67922538
8	*A*	0·92788625	−0·45968254	−0·83958844	0·59847660
	B	0·92788575	−0·45966503	−0·84020153	0·61993917
9	*A*	0·94337616	0·02994267	−0·96084986	0·52905581
	B	0·94337557	0·02996296	−0·96155178	0·55333614
10	*A*	−0·48812323	−0·51496366	0·99905101	−0·45387716
	B	−0·48812260	−0·51471526	0·99979004	−0·47915465
11	*A*	0·21382391	−0·86976010	0·94750077	−0·37290634
	B	0·21382453	−0·86978115	0·94821361	−0·39704369
12	*A*	−0·80974456	0·99998041	−0·80730487	0·28621358
	B	−0·80974511	0·99999880	−0·80792250	0·30695232
13	*A*	−0·99461913	0·86659758	−0·58846691	0·19428656
	B	−0·99461954	0·86661126	−0·58892335	0·20951759
14	*A*	0·66990631	−0·50112309	0·31026401	−0·09827506
	B	0·66990653	−0·50113039	0·31050683	−0·10634633

($k = 1$ or 2) are of the order 10^{15} for tungsten, and 10^{24} for iron. It can be shown that the influence of the surface component diminishes as the magnitude of $(C_{12} - C_{44})$, which corresponds to the force constant γ_1 of angular interaction, decreases. In order to show the influence of the surface component and the difference between the mode shapes in the [100] direction and those in the [110] direction, we have plotted the mode shapes of the latter for $\theta = 0{\cdot}2\pi$, in Fig. 17, and tabulated the normalized displacements in Tables 11 and 12, both with and without the contribution of the surface component.

The similarity between the propagations of face-shear and thickness-twist waves in a b.c.c. crystal lattice plate in the [110] direction and in a simple cubic or f.c.c. plate in the [100] direction is not an unexpected coincidence. This similarity, as well as the difference between the propagations of the face-shear and thickness-twist waves in a b.c.c. crystal lattice plate in the [100] direction and in the [110] direction can be accounted for as follows. Consider a crystal lattice plate: the normal to the plane of the plate is in the x_3-direction,

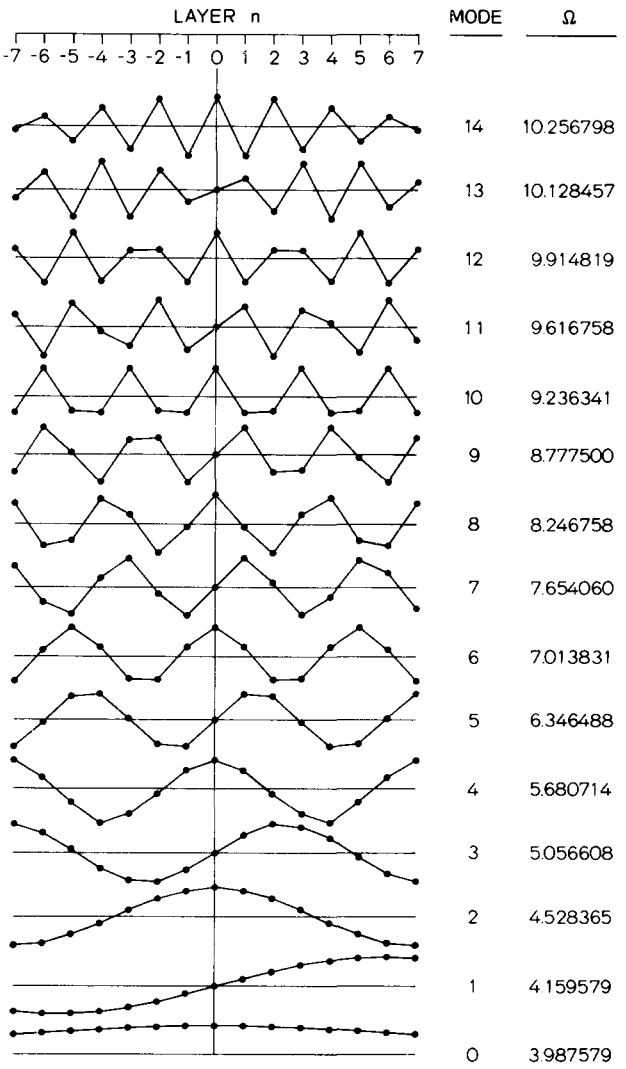

FIG. 17. Mode shapes and normalized frequencies of face-shear and thickness-twist waves along the [110] direction with $\theta = 0{\cdot}2\pi$ in a plate 15 atomic layers thick (tungsten).

the wave-normal of the face-shear and thickness-twist waves is in the x_1-direction, the displacement vector is parallel to the x_2-direction. As the waves propagate in the plate, we observe that the motion of the atoms in each atomic layer is independent of the position of the atoms in the x_2-direction. Therefore, the wave motion in such a plate is essentially equivalent to the wave motion in a plane lattice strip which is actually the projection of the plate in an $x_1 - x_3$ plane.

We have already shown that the geometrical configuration of a b.c.c. crystal lattice viewed from the [110] direction is similar to that of an f.c.c. crystal lattice, and that the

TABLE 11. THE NORMALIZED DISPLACEMENTS OF THE LAYERS WITH $0 \leq n \leq 3$, (UPON WHICH THE SURFACE COMPONENTS OF THE DISPLACEMENTS HAVE NEGLIGIBLE INFLUENCE) FOR THE FACE-SHEAR AND THICKNESS-TWIST WAVES PROPAGATING IN THE [110] DIRECTION, WITH $\theta = 0{\cdot}2\pi$ IN A PLATE 15 ATOMIC LAYERS THICK (TUNGSTEN)

Mode	Layer n			
	0	1	2	3
0	1·00	0·99423130	0·97699176	0·94848027
1	0·00	0·25992856	0·51098851	0·70953961
2	1·00	0·89998606	0·61994981	0·21590631
3	0·00	0·60588017	0·96402311	0·92798841
4	1·00	0·65599353	−0·13934497	−0·83881233
5	0·00	0·87331922	0·85087208	−0·04431733
6	1·00	0·29637110	−0·82432834	−0·78498529
7	0·00	0·99574782	0·18345859	−0·96194703
8	1·00	−0·11645118	−0·97287824	0·34303683
9	0·00	0·94742530	−0·60630868	−0·55941560
10	1·00	−0·50937378	−0·48107671	0·99946951
11	0·00	0·73659899	−0·99636762	0·61114714
12	1·00	−0·81371640	0·32426877	0·28599076
13	0·00	0·40145935	−0·73537464	0·94556586
14	1·00	−0·97877106	0·91598559	−0·81430931

propagation of the face-shear and thickness-twist waves in a b.c.c. crystal lattice along the [110] direction is almost identical with that in an f.c.c. crystal lattice along the [100] direction. Now, according to the above observation which reduces the wave-motion to that in a lattice strip, we find that the projected plane lattice strip of an f.c.c. crystal lattice plate is identical with that of a simple cubic crystal lattice. Thus we may expect that the thickness-twist wave motions for both plates along the [100] direction will be similar. Consequently, the dispersion spectra of face-shear and thickness-twist waves in the simple cubic crystal lattice plate and the f.c.c. crystal lattice plate in the [100] direction and in the b.c.c. crystal lattice plate in the [110] direction are all alike, except for the existence of a small contribution by the surface component of displacements in the f.c.c. as well as the b.c.c. crystal lattice plates. The surface components are due to the long interlayer interactions considered in this paper as well as in Ref. [2].

The atoms in a plane projection of a b.c.c. crystal lattice along the [010] direction form a centered square lattice. For waves propagating in the x_1-direction the atoms in adjacent layers have a spatial phase difference along the x_1-direction which separates the atoms in alternating atomic layers into two groups. For each vibrational mode across the thickness of the strip, we may regard the mass centers of the two groups of atoms as two distinct mass points in a one dimensional diatomic lattice. Thus the mode will correspond to an acoustical mode if the neighboring particles are in phase, and an optical mode if the neighboring particles move in opposite directions. This situation provides a physical explanation for the substantial difference in the character of the dispersion curves for waves along the [100] and [110] directions, in the b.c.c. lattice.

TABLE 12. THE NORMALIZED DISPLACEMENTS OF THE LAYERS WITH $4 \leq n \leq 7$. (A) WITH AND (B) WITHOUT THE CONTRIBUTION OF THE SURFACE COMPONENT OF THE DISPLACEMENT. THE FACE-SHEAR AND THICKNESS-TWIST WAVES ARE PROPAGATING IN THE [110] DIRECTION WITH $\theta = 0{\cdot}2\pi$ IN A PLATE 15 ATOMIC LAYERS THICK (TUNGSTEN)

Mode		Layer n			
		4	5	6	7
0	A	0·90902579	0·85908329	0·79923999	0·72964611
	B	0·90902578	0·85908351	0·79922964	0·73015474
1	A	0·86831392	0·96739596	1·00000647	0·96233012
	B	0·86831391	0·96739658	0·99997624	0·96381325
2	A	−0·23132450	−0·63228246	−0·90684004	−0·99639475
	B	−0·23132447	−0·63228391	−0·90676893	−0·99987488
3	A	0·51251017	−0·11252458	−0·69168747	−0·98129672
	B	0·51251023	−0·11252732	−0·69155378	−0·98781208
4	A	−0·96116587	−0·42222937	0·40742563	0·94614305
	B	−0·96116596	−0·42222497	0·40721226	0·95648219
5	A	−0·89405017	−0·82675928	0·08885091	0·89842851
	B	−0·89405030	−0·82675298	0·08854757	0·91302458
6	A	0·35903426	0·99780843	0·23200848	−0·84117294
	B	0·35903444	0·99780015	0·23240382	−0·86004460
7	A	−0·36068987	0·89550299	0·52519700	−0·77592084
	B	−0·36068965	0·89549285	0·52567706	−0·79864105
8	A	0·89298440	−0·55102663	−0·76410383	0·70341464
	B	0·89298415	−0·55101496	−0·76465146	0·72910410
9	A	0·96430923	−0·05771050	−0·92679688	0·62383287
	B	0·96430896	−0·05769785	−0·92738499	0·65118165
10	A	−0·53713068	−0·45225637	0·99728610	−0·53699047
	B	−0·53713040	−0·45226921	0·99787856	−0·56431713
11	A	0·16969338	−0·84067276	0·96691283	−0·44260607
	B	0·16969365	−0·84068486	0·96746671	−0·46796817
12	A	−0·78969930	0·99918184	−0·83594909	0·34065499
	B	−0·78969953	0·99919215	−0·83641856	0·36202286
13	A	−0·99666894	0·88007891	−0·61509060	0·23174270
	B	−0·99666911	0·88008646	−0·61543250	0·24723430
14	A	0·67805911	−0·51301614	0·32601897	−0·11737970
	B	0·67805920	−0·51302013	0·32619932	−0·12552878

Acknowledgments—The author is indebted to Professor R. D. Mindlin and Dr. D. C. Gazis for valuable advice. The work was supported by the Office of Naval Research under a contract with Columbia University.

REFERENCES

[1] R. D. MINDLIN, Lattice theory of shear modes of vibration and torsional equilibrium of simple cubic crystal plates and bars. *Int. J. Solids Struct.* **6**, 725–738 (1970).

[2] K. J. BRADY, Lattice theory of face-shear and thickness-twist waves in f.c.c. crystal plates. *Int. J. Solids Struct.* to be published.

[3] B. C. CLARK, D. C. GAZIS and R. F. WALLIS, Frequency spectra of body-centered cubic lattices. *Phys. Rev.* **134**, A1486–A1491 (1964).

[4] T. E. FEUCHTWANG, Dynamics of a semi-infinite crystal lattice in a quasiharmonic approximation—II. The normal-mode analysis of a semi-infinite lattice, *Phys. Rev.* **155**, 731–744 (1967).

[5] R. E. ALLEN, G. P. ALLDREDGE and F. W. DE WETTE, Surface modes of vibration in monatomic crystals. *Phys. Rev. Lett.* **23**, 1285–1287 (1969).

[6] D. C. GAZIS and R. F. WALLIS, Surface elastic waves in body-centered cubic lattices. *Surf. Sci.* **5**, 482–492 (1966).
[7] LORD RAYLEIGH, *The Theory of Sound*, Vol. I, Chapter IV, Sec. 88–89, pp. 109–113. MacMillan (1929).
[8] J. A. RAYNE and B. S. CHANDRASEKHAR, Elastic constants of iron from 4·2 to 300°K. *Phys. Rev.* **122**, 1714–1716 (1961).
[9] W. B. PEARSON, *A Handbook of Lattice Spacings and Structures of Metals and Alloys*, Vols. 1 and 2. Pergamon Press (1958, 1967).
[10] V. J. MINKIEWICZ, G. SHIRANE and R. NATHANS, Phonon dispersion relation for iron (α-Fe). *Phys. Rev.* **163**, 528–531 (1967).
[11] F. H. FEATHERSTON and J. R. NEIGHBOURS, Elastic constants of tantalum, tungsten and molybdenum. *Phys. Rev.* **130**, 1324–1333 (1963).
[12] S. H. CHEN and B. N. BROCKHOUSE, Lattice vibrations of tungsten. *Solid St. Communs* **2**, 73–77 (1964).
[13] D. C. GAZIS, R. HERMAN and R. F. WALLIS, Surface elastic waves in cubic crystals. *Phys. Rev.* **119**, 533–544 (1960).
[14] R. D. MINDLIN, Lecture Notes (1966).
[15] R. D. MINDLIN, An introduction to the mathematical theory of vibrations of elastic plates, U.S. Army Signal Corps Engineering Laboratories, Fort Monmouth, New Jersey (1955).

(*Received* 1 *November* 1970)

Абстракт—Дается аналитическое исследование волн сдвига грани и сдвига по толщине, которые распространяются вдоль направлений [100] и [110] пластинки с объемноцентрированнои кубической решеткой и ограниченной парой поверхностей (001). Поведение этих волн для направления [110] подобно такому же, найденному ранее для подобных волн, направленных по [100] для пластинок с простой кубической и гранецентрированной решеткой. Совершенно разная ситуация вдоль направления [100] пластинки с объемноцентрированной кубической решеткой. Вблизи точки лежащей на полпути первой зоны · Бриллюэна, самый низкий симметрический и самый низкий антисимметрический вид колебаний оказываются преобладающими видами колебаний поверхности. Остальные виды колебаний группируются вместе в узкой, пропускающей полосе высокой частоты. Приводятся результаты численных расчетов для железа и вольфрама.